

Electronic Supporting Information (ESI)

Access to highly active Ni-Pd bimetallic nanoparticle catalysts for C-C coupling reactions

Rohit K. Rai,^a Kavita Gupta,^a Deepika Tyagi,^a Arup Mahata,^a Silke Behrens,^b Xinchun Yang,^c Qiang Xu,^c Biswarup Pathak^a and Sanjay K. Singh^{*a,d}

^a*Discipline of Chemistry, Indian Institute of Technology (IIT) Indore, Simrol, Indore, 452020, India*

^b*Institute of catalysis Research and Technology (IKFT), Karlsruhe Institute of Technology (KIT), Hermann-von-Helmholtz-Platz 1, 76344 Eggenstein-Leopoldshafen, Germany*

^c*National Institute of Advanced Industrial Science and Technology (AIST), Ikeda, Osaka 563-8577, Japan*

^d*Centre for Material Science and Engineering, Indian Institute of Technology (IIT) Indore, Simrol, Indore, 452020, India*

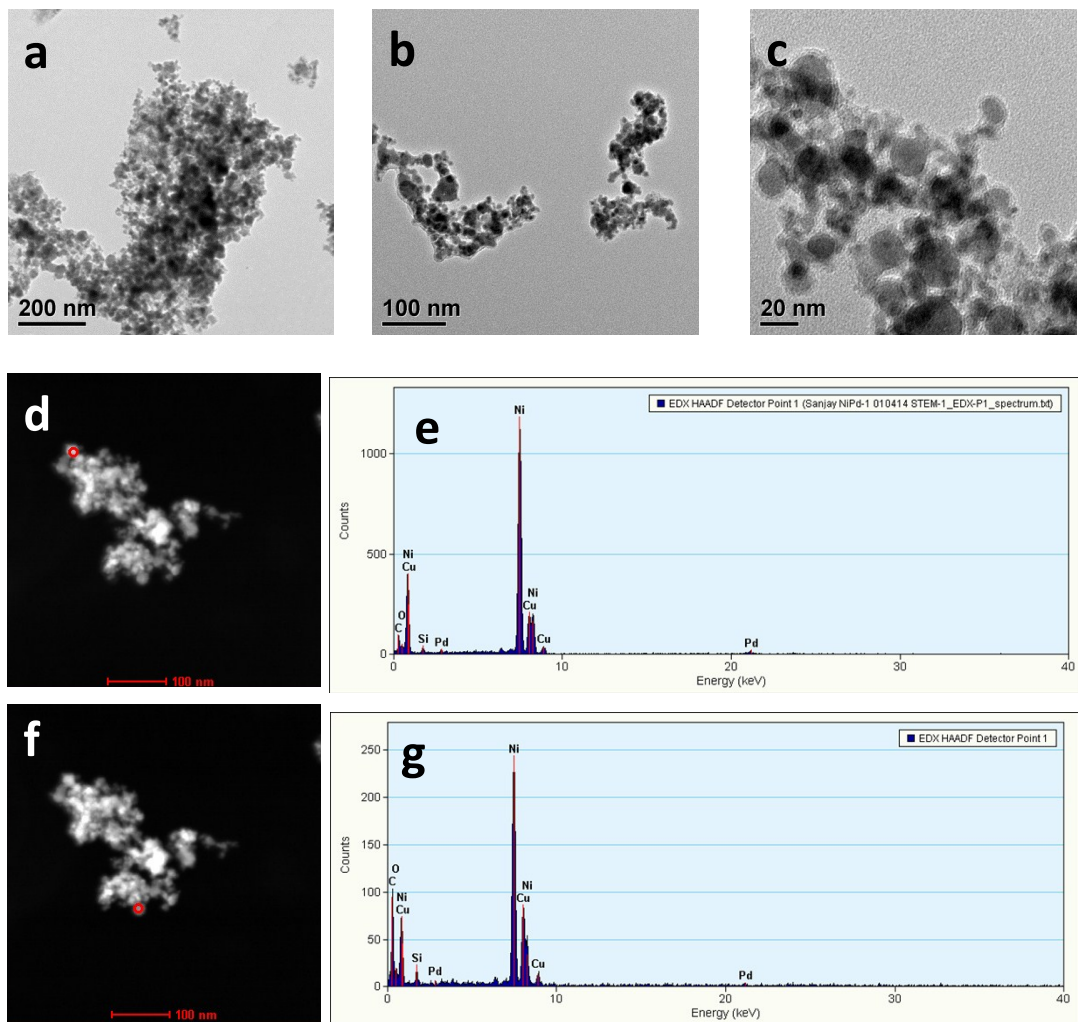


Figure S1. Characterization of $\text{Ni}_{0.99}\text{Pd}_{0.01}$ nanoparticle catalyst. (a-c) TEM images. (d-g) HAADF-STEM images with corresponding EDX point scan profiles.

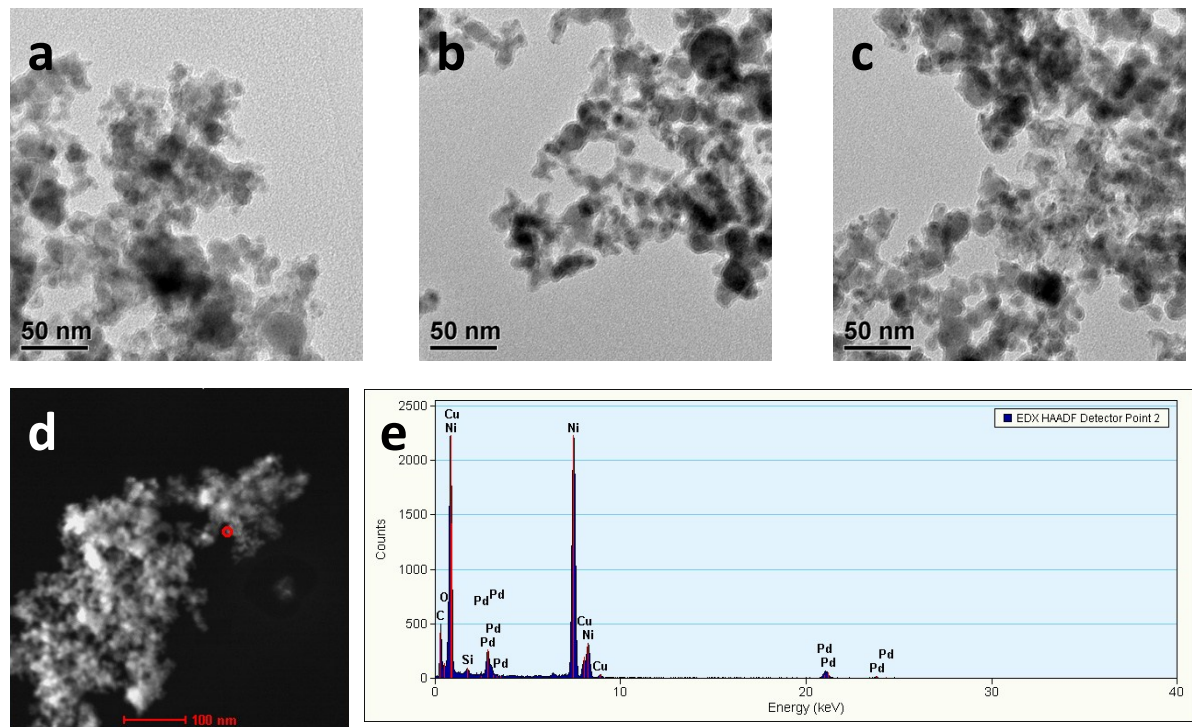


Figure S2. Characterization of $\text{Ni}_{0.95}\text{Pd}_{0.05}$ nanoparticle catalyst. (a-c) TEM images. (d-e) HAADF-STEM image with corresponding EDX point scan profile.

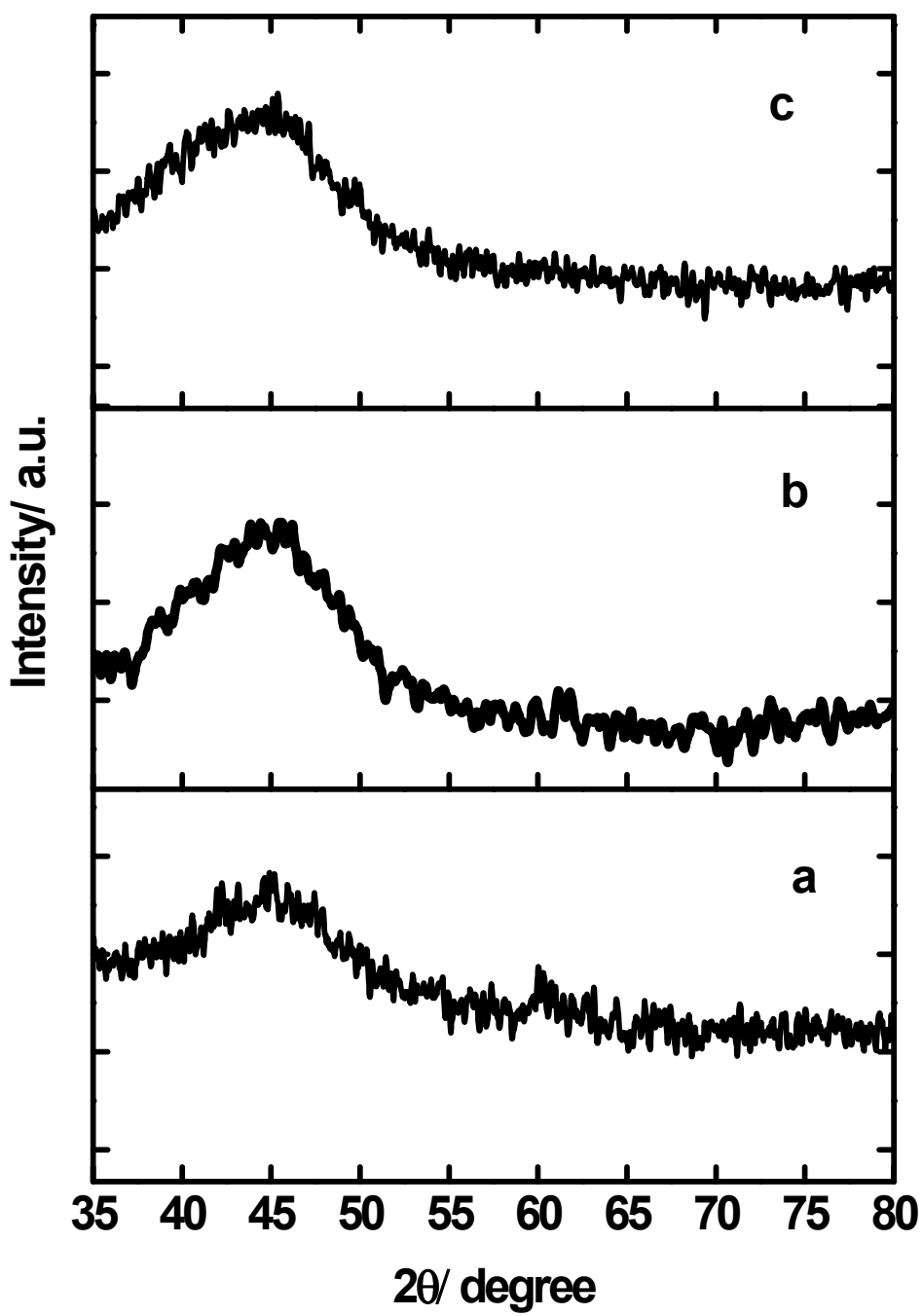


Figure S3. Powder XRD profile of a) Ni, b) $\text{Ni}_{0.99}\text{Pd}_{0.01}$ and c) $\text{Ni}_{0.95}\text{Pd}_{0.05}$ nanoparticle catalysts.

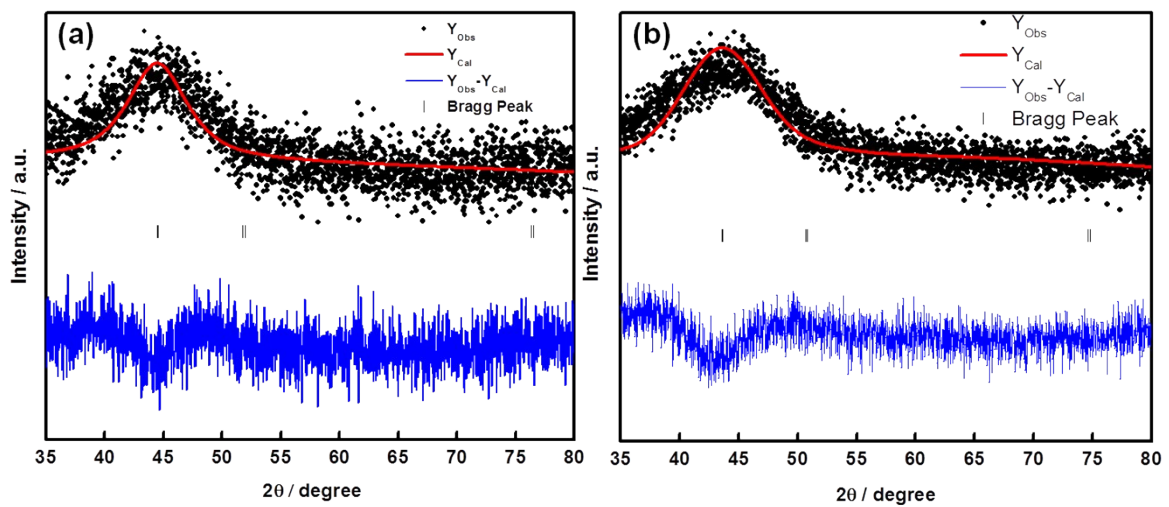


Figure S4. Representative Le Bail fit of an X-ray diffraction spectrum of a) $\text{Ni}_{0.99}\text{Pd}_{0.01}$ and b) $\text{Ni}_{0.95}\text{Pd}_{0.05}$ nanoparticle catalyst.

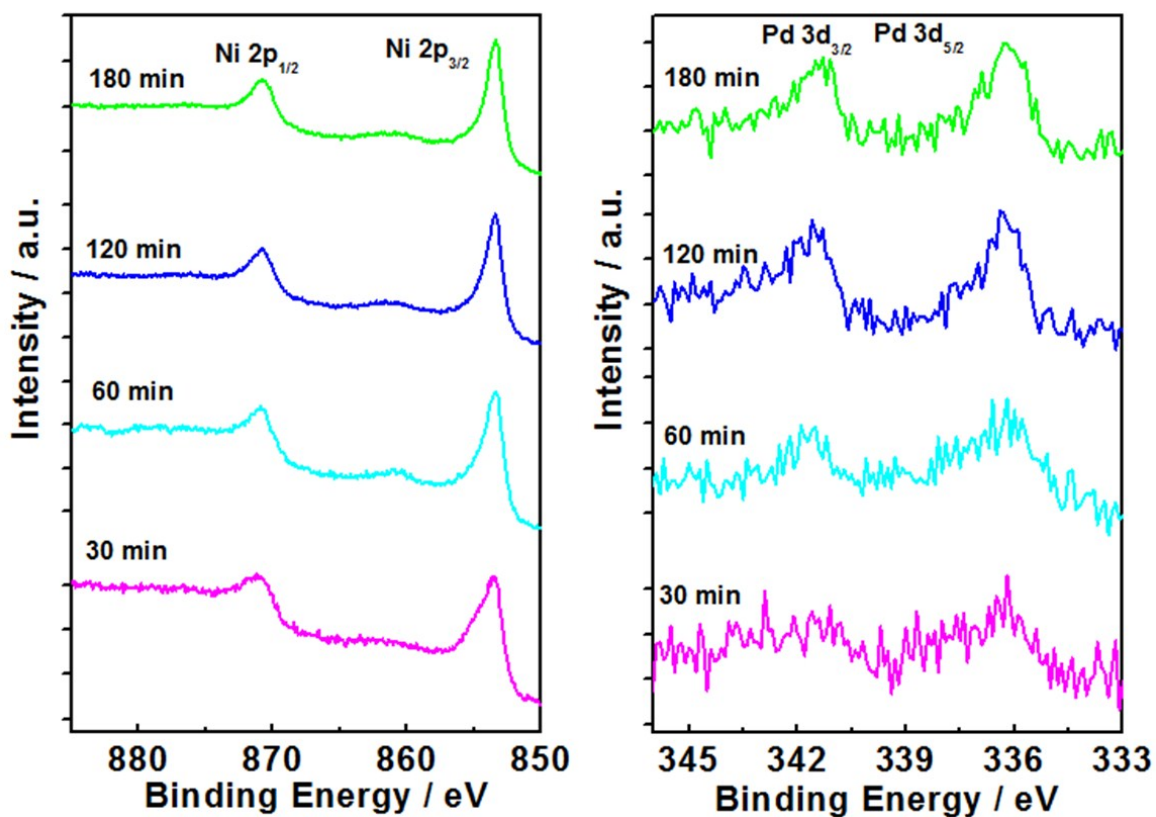


Figure S5. XPS profiles of Ni-L and Pd-K edge for $\text{Ni}_{0.99}\text{Pd}_{0.01}$ nanoparticle catalyst.

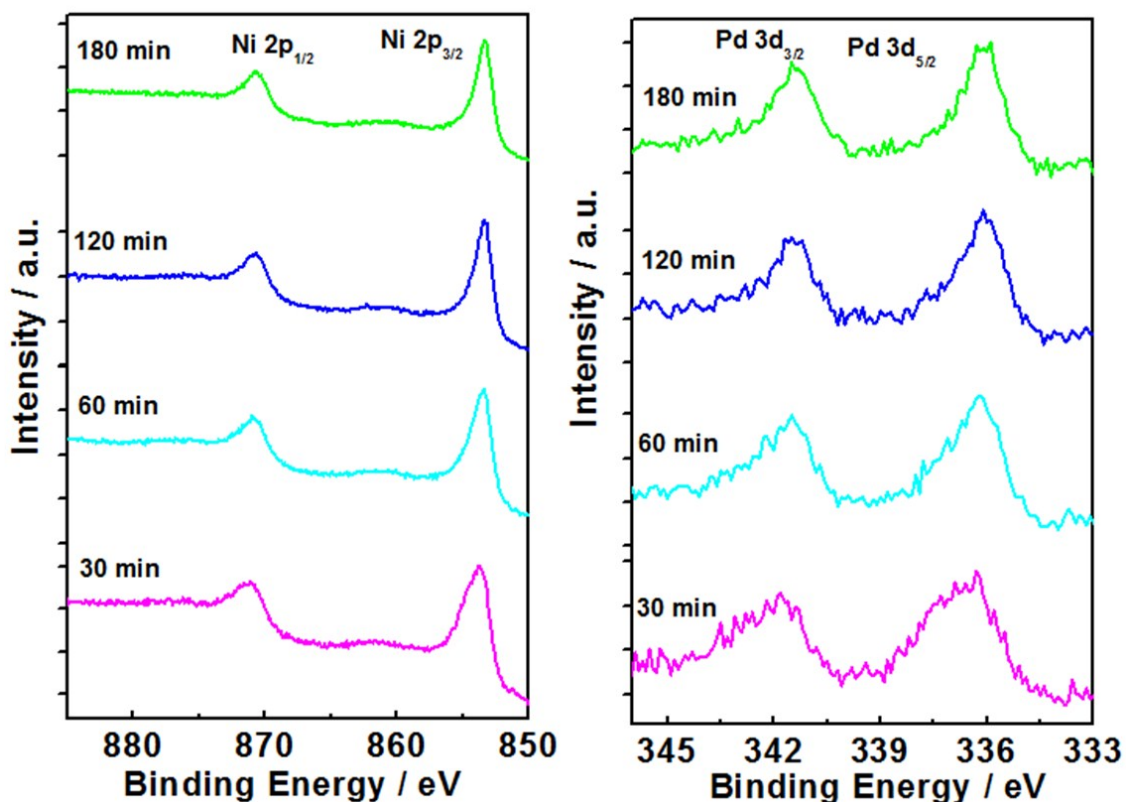


Figure S6. XPS profiles of Ni-L and Pd-K edge for $\text{Ni}_{0.95}\text{Pd}_{0.05}$ nanoparticle catalyst.

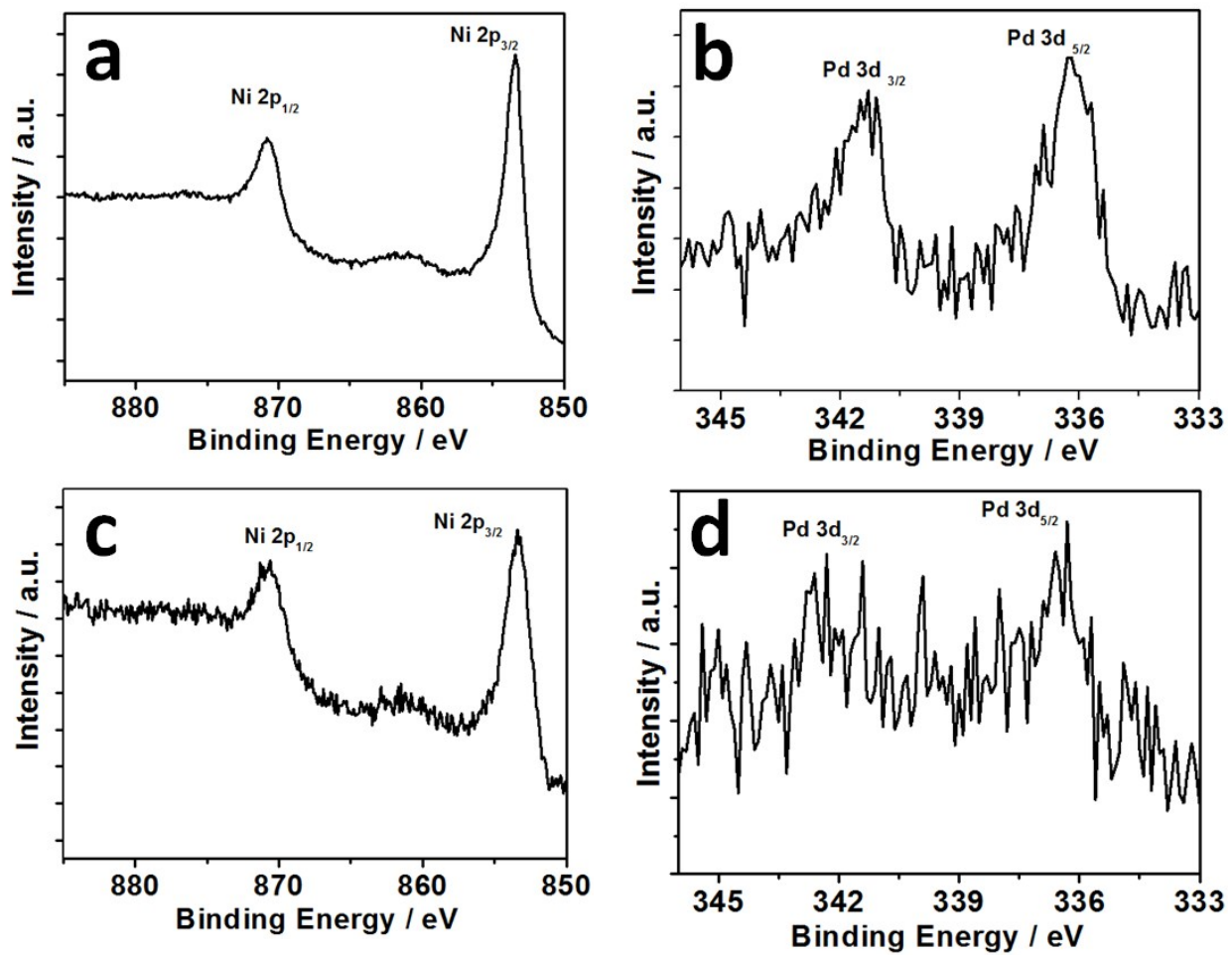


Figure S7. XPS profiles corresponding to the $\text{Ni}_{2\text{p}}$ and $\text{Pd}_{3\text{d}}$ core levels of the $\text{Ni}_{0.99}\text{Pd}_{0.01}$ nanoparticle catalyst, (a, b) before and (c, d) after the catalytic Suzuki-Miyaura reaction at rt.

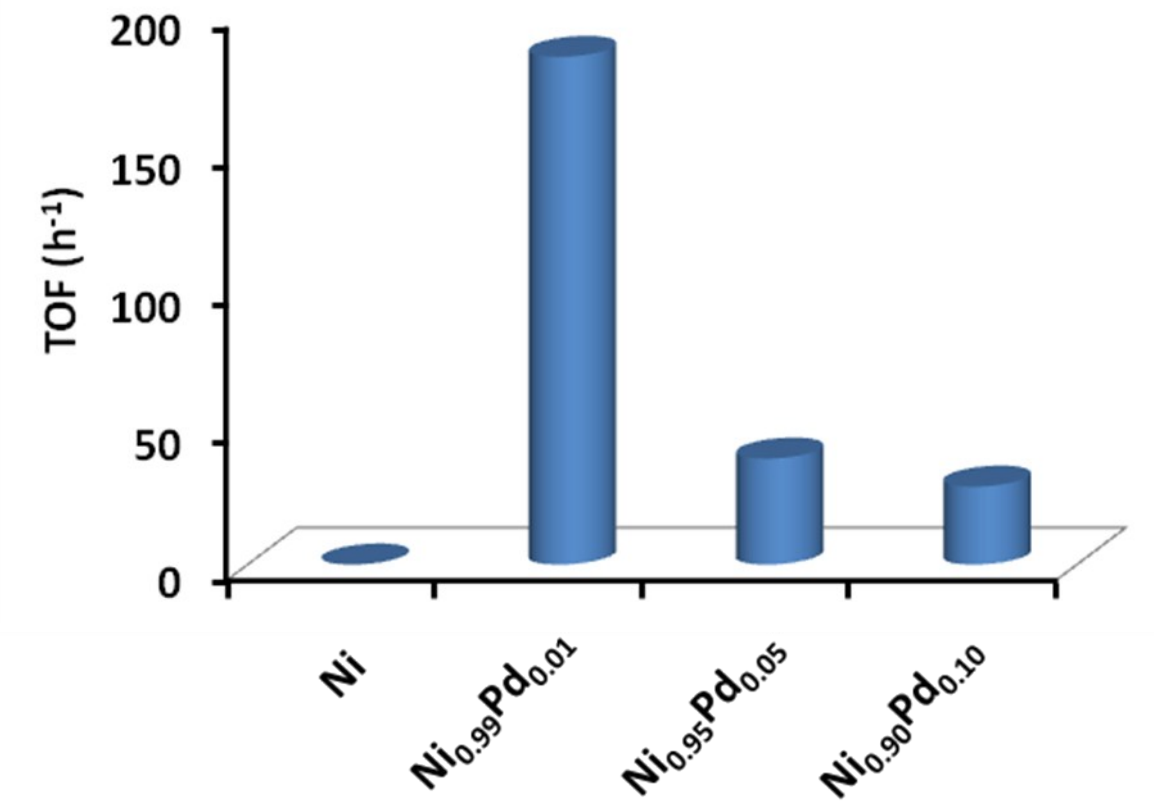


Figure S8. Comparison of catalytic conversions for cross-coupled product in the Heck reaction of 4-iodotoluene and styrene in presence of 2 mol % of various catalysts at 80 °C in DMF/H₂O (1:1 v/v, 5 mL) for 14 h.

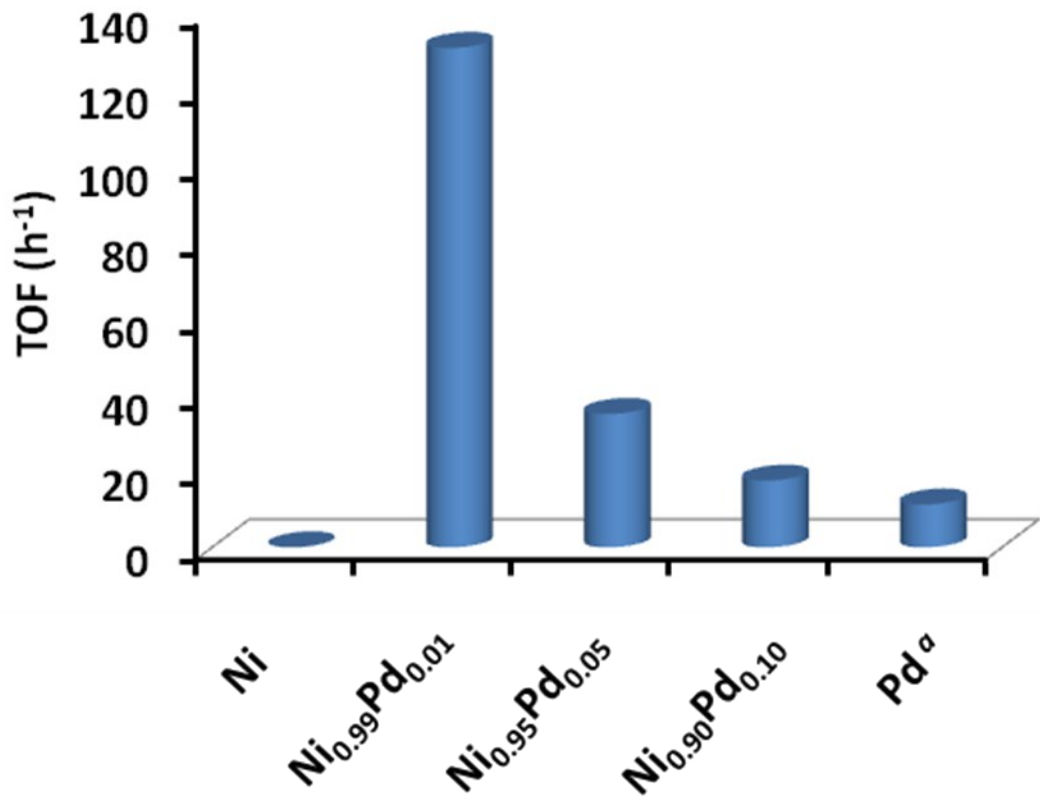


Figure S9. Comparison of catalytic conversions for cross-coupled product in the Sonogashira reaction of 4-iodotoluene and phenylacetylene in presence of 2 mol% of various catalysts at 80 °C in DMF/H₂O (1:1 v/v, 5 mL) for 12 h. (^a Reaction with 0.1 mol % Pd, equal to the Pd content present in highly active 2 mol % $\text{Ni}_{0.95}\text{Pd}_{0.05}$ nanocatalyst).

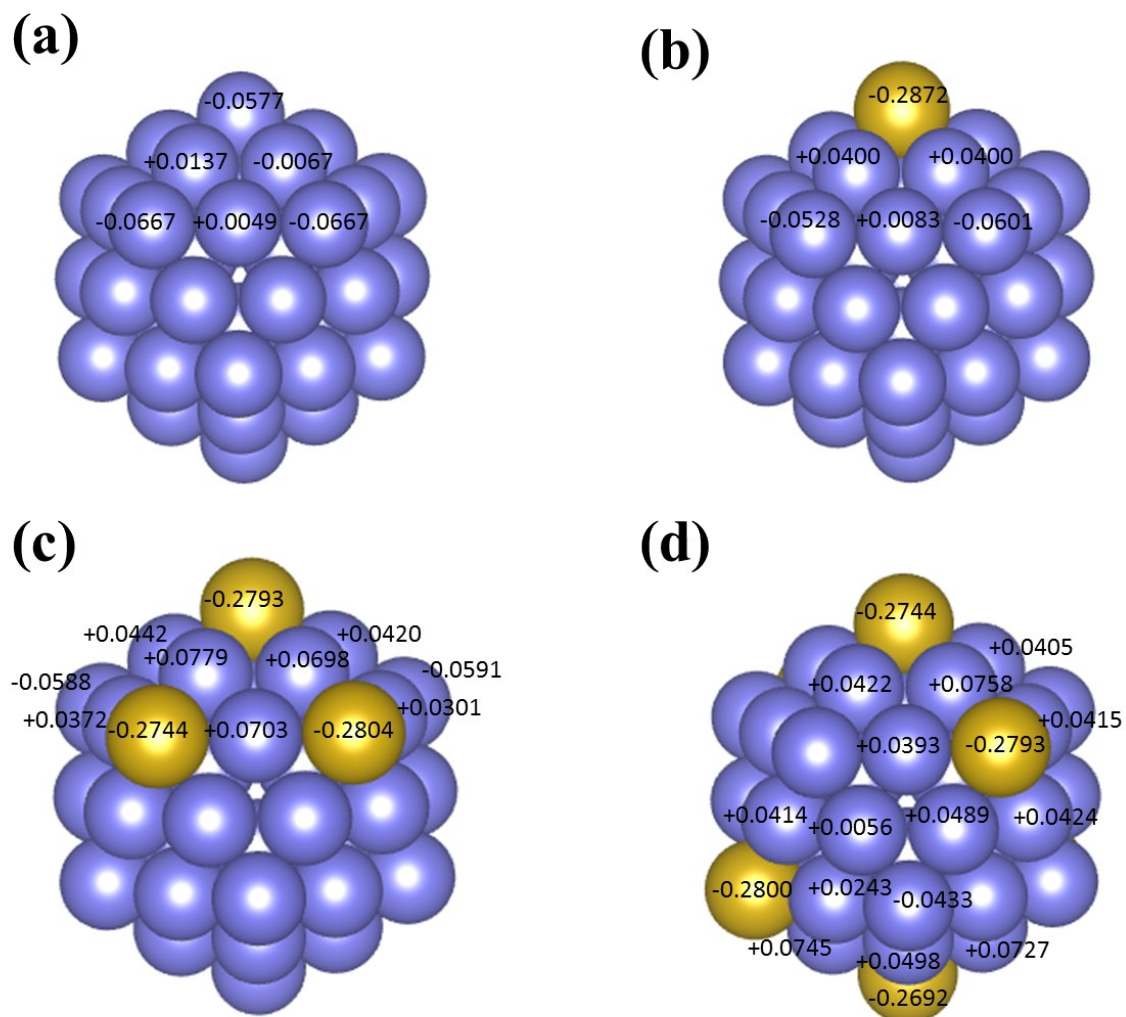


Figure S10. Optimized structures of icosahedral (a) Ni_{55} , (b) $\text{Ni}_{54}\text{Pd}_1$, (c) $\text{Ni}_{52}\text{Pd}_3$ and (d) $\text{Ni}_{49}\text{Pd}_6$ clusters showing the net accumulated Bader charges on Ni (in blue) and Pd (in golden yellow) atoms.

The charge density difference (CDD)^{S1-S2} is plotted to understand the nature of bonding between the pure and doped nanocluster. The CDD is calculated using the following equation:

$$\rho_{\text{CDD}} = \rho^{\text{total}} - \sum \rho_i^{\text{fragments}}$$

Here the ρ^{total} is the total charge density of the system and $\rho_i^{\text{fragments}}$ is the charge density of the individual fragments by which the system is made of. Here the charge density of the fragments ($\rho_i^{\text{fragments}}$) is calculated by a pseudo structure in which fragment part retains the same structure as in the total system but other parts are deleted. Here, we have mainly two different fragments, the Ni cluster and Pd atoms. In CDD, the positive and negative charge density is plotted by red and green colours respectively.

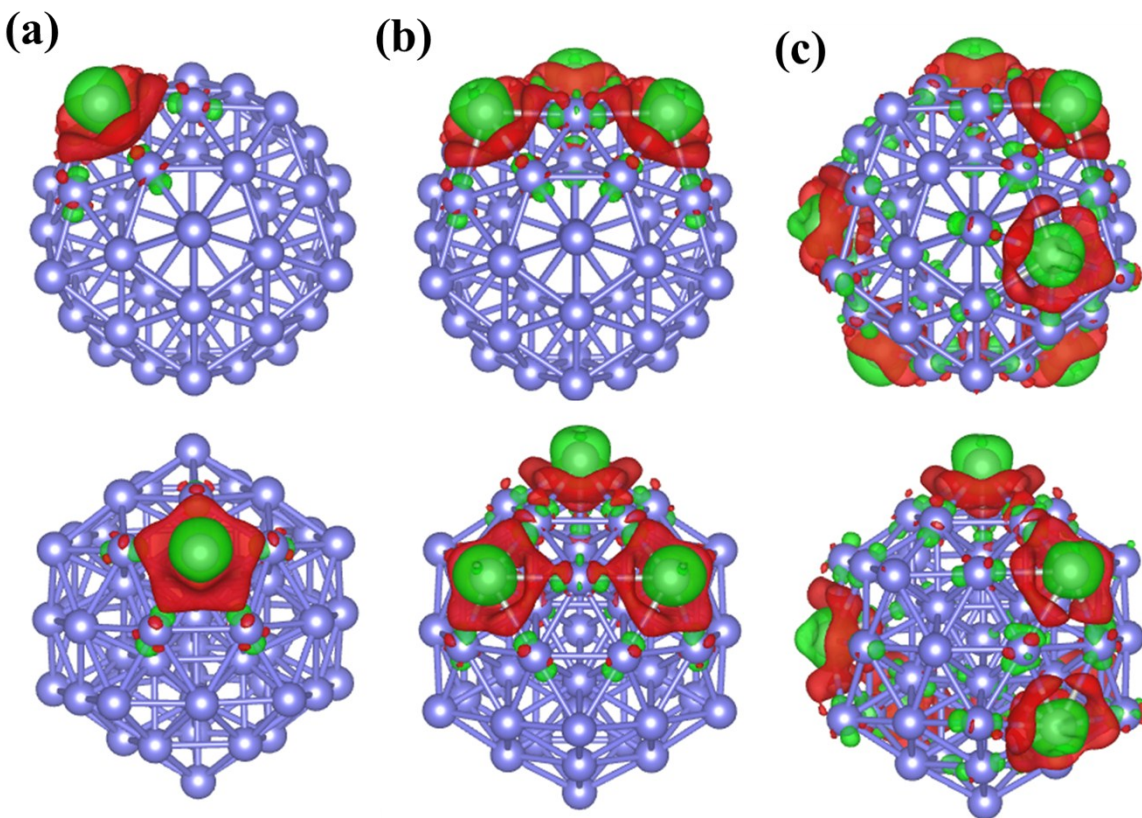


Figure S11. The CDD plot of icosahedral (a) $\text{Ni}_{54}\text{Pd}_1$, (b) $\text{Ni}_{52}\text{Pd}_3$ and (c) $\text{Ni}_{49}\text{Pd}_6$ (Isosurface value = 0.005 e Å⁻³) clusters, showing positive (in red) and negative (in green) charge densities. Upper and lower stair represents the side and top view respectively.

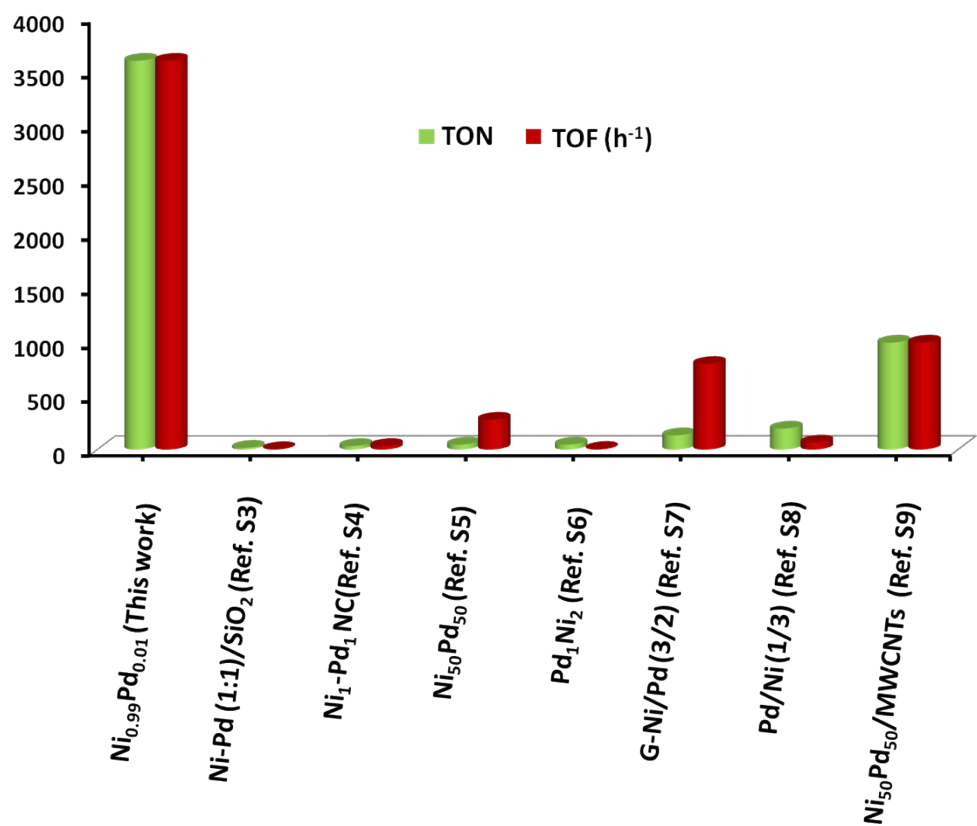


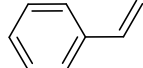
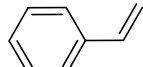
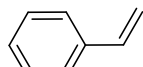
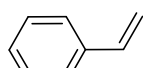
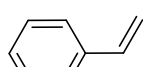
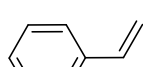
Figure S12. Comparative highest TON and TOF (h^{-1}) on the basis of Pd of the different Ni-Pd nanoparticle catalysts for Suzuki reaction.

Table S1. ICP-AES data for the Ni-Pd nanoparticle catalyzed Suzuki-Miyaura reaction.^a

Entry	Catalytic runs	Ni to Pd atomic ratio	Leaching Pd (ppm)
1	1 st	94.9/5.1	0.16
2	2 nd	94.8/5.2	nil
3	7 th	97/3	nd
4 ^b	1 st	93.3/6.7	0.13
5 ^c	1 st	99.4/0.6	0.17
6 ^d	1 st	99.3/0.7	0.06
7 ^e	2 nd	98.9/1.1	0.05

^a Reaction condition: 2-methylphenylboronic acid (1.2 mmol), 4-iodoanisole (1.0 mmol), catalyst (2 mol %), NaOH (2.0 mmol), H₂O-C₂H₅OH (1:1 v/v, 20 mL).^b With Ni_{0.95}Pd_{0.05} at 50 °C, ^c With Ni_{0.99}Pd_{0.01} at 50 °C, and ^{d,e} With Ni_{0.99}Pd_{0.01} at rt.

Table S2. Optimization of Heck reaction by $\text{Ni}_{0.95}\text{Pd}_{0.05}$ nanoparticle catalyst. ^a

Entry	Arylhalides	Styrene	Styrene (mmol)	Base	Solvent	Conv./Sel. (%) ^b
1			1.2	Et_3N	$\text{H}_2\text{O}-\text{C}_2\text{H}_5\text{OH}$	3/99
2			1.5	Et_3N	$\text{H}_2\text{O}-\text{C}_2\text{H}_5\text{OH}$	20/99
3			1.5	K_3PO_4	$\text{H}_2\text{O}-\text{C}_2\text{H}_5\text{OH}$	20/99
4			1.5	K_2CO_3	$\text{H}_2\text{O}-\text{C}_2\text{H}_5\text{OH}$	32/99
5			1.5	Et_3N	$\text{H}_2\text{O}-\text{DMF}$	46/99
6			1.5	K_2CO_3	$\text{H}_2\text{O}-\text{DMF}$	90/99

^a Reaction condition: arylhalide (1.0 mmol), styrene, catalyst (2 mol %), base (2.0 mmol), solvent (1:1 v/v, 5 mL), 80 °C, 24 h. ^b Conversion and selectivity were determined by ¹H NMR.

Table S3. Heck reaction with Ni_{0.95}Pd_{0.05} alloy nanoparticle catalyst.^a

Entry	Arylboromides	Arylalkene	Time (h)	Conv./Sel. (%)
1			24	79/82(7)
2			24	60/54(11)
3			24	99/67(10)
4			24	99/43(8)

^a Reaction condition: arylhalides (1.0 mmol), arylalkene (1.5 mmol) K₂CO₃ (2.0 mmol), H₂O-DMF (1:1 v/v, 5 mL), catalyst (2 mol%), 110 °C. Isolated yields in parentheses.

Table S4. Sonogashira reaction with Ni_{0.95}Pd_{0.05} alloy nanoparticle catalyst.^a

Entry	Arylalkyne	Arylhalides	Time (h)	Conv./Sel. (%)
1			24	30/99(20)
2			24	9/99(8)

^a Reaction condition: arylhalides (1.0 mmol), arylalkyne (1.0 mmol), K₂CO₃ (2.0 mmol), CuI (2 mol %) H₂O-DMF (1:1 v/v, 5 mL), catalyst (2 mol %), at 80 °C. Isolated yields in parentheses.

Table S5. Sonogashira reaction with $\text{Ni}_{0.95}\text{Pd}_{0.05}$ alloy nanoparticle catalyst.^a

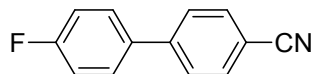
Entry	Arylalkyne	Arylhalides	Time (h)	Conv./Sel. (%)
1			24	40/64(8)
2			24	51/74(11)
3			24	99/60(7)

^a Reaction condition: arylhalides (1.0 mmol), arylalkyne (1.0 mmol), KO^tBu (2.0 mmol), H_2O -DMF (3:2 v/v, 5 mL), catalyst (2 mol%), 110 °C. Isolated yields in parentheses.

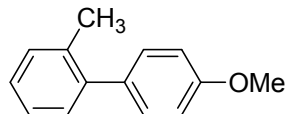
Table S6. Comparative catalytic activity, in terms of TON and TOF (h^{-1}), of the reported $\text{Ni}_{0.99}\text{Pd}_{0.01}$ catalyst with various other heterogeneous Pd catalysts for Suzuki reaction.

Entry	Catalyst	Reaction conditions	TON/TOF(h^{-1})	Ref.
1	Ni–Pd	$\text{C}_2\text{H}_5\text{OH}-\text{H}_2\text{O}$, 50 °C	3600/3600	This work
2	Pd–Im–Phos– $\text{SiO}_2@\text{Fe}_3\text{O}_4$	$\text{C}_2\text{H}_5\text{OH}-\text{H}_2\text{O}$, 60 °C	320/320	S10
3	PFG–Pd	$\text{C}_2\text{H}_5\text{OH}-\text{H}_2\text{O}$, K_2CO_3 , 80 °C	81/405	S11
4	Pd/ Fe_3O_4 /s–G	$\text{C}_2\text{H}_5\text{OH}-\text{H}_2\text{O}$, K_2CO_3 , 80 °C	317/422	S12
5	Pd/TiO ₂	NMP– H_2O , Na_2CO_3 , 120 °C	140/35	S13
6	Pd NPs–rGO	$\text{C}_2\text{H}_5\text{OH}-\text{H}_2\text{O}$, K_2CO_3 , RT	11/5	S14
7	G/MWCNTs/Pd	$\text{C}_2\text{H}_5\text{OH}-\text{H}_2\text{O}$, K_2CO_3 , 60 °C	198/792	S15
8	Pd/CNT–SiC monolith	$\text{C}_2\text{H}_5\text{OH}-\text{H}_2\text{O}$, K_3PO_4 , 60 °C	1800/1800	S16
9	Pd–slGO–60	$\text{C}_2\text{H}_5\text{OH}-\text{H}_2\text{O}$, K_3PO_4 , RT	9900/9900	S17
10	Pd/ Fe_3O_4	CH_3OH , K_3PO_4 , 60 °C	950/79	S18
11	Pd/MWCNT	$\text{C}_2\text{H}_5\text{OH}-\text{H}_2\text{O}$, K_2CO_3 , 80 °C, MW	200/1200	S19
12	Pd@ZPGly-15	$\text{C}_2\text{H}_5\text{OH}$, K_2CO_3 , 70 °C	980/98	S20
13	Pd/SBA-15	DMF– H_2O , 110 °C	1996/1996	S21
14	CelMcPd0-1	$\text{C}_2\text{H}_5\text{OH}$, K_2CO_3 , reflux	188/1128	S22
15	Pd@pSiO ₂	DMF– H_2O , 200 °C	33333/11111	S23
16	Pd/NiFe ₂ O ₄	DMF– H_2O , Na_2CO_3 , 90 °C	970/11640	S24
17	Fe@ Fe_xO_y /Pd	$\text{C}_2\text{H}_5\text{OH}-\text{H}_2\text{O}$, K_2CO_3 , RT	198/99	S25
18	Alginate/Cu ²⁺ /Pd	$\text{C}_2\text{H}_5\text{OH}$, K_2CO_3 , 70 °C	990000/38076	S26
19	Pd–PVP–Fe	$\text{C}_2\text{H}_5\text{OH}-\text{H}_2\text{O}$, TBAB, reflux	177/354	S27
20	Pd–ScBTC NMOFs	$\text{C}_2\text{H}_5\text{OH}-\text{H}_2\text{O}$, K_2CO_3 , 40 °C	194/388	S28
21	Pd/IL–NH ₂ /SiO ₂ / Fe_3O_4	$\text{C}_2\text{H}_5\text{OH}-\text{H}_2\text{O}$, NaOH, RT	196/65	S29
22	GO–PdP ₂ /GO–Pd ₄ S	$\text{C}_2\text{H}_5\text{OH}-\text{H}_2\text{O}$, K_2CO_3 , 80 °C	192/384	S30
23	PVP–Pd NP	$\text{C}_2\text{H}_5\text{OH}-\text{H}_2\text{O}$, K_3PO_4 , 90 °C	123750/61875	S31

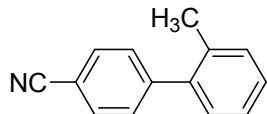
Spectral data of the coupled products



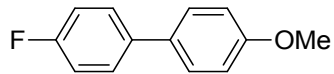
4-Cyano, 4'-fluorobiphenyl: **$^1\text{H NMR}$ (400 MHz, CDCl_3 , ppm):** $\delta = 7.72$ (d, 2H, $J = 8\text{Hz}$),
 7.64 (d, 2H, $J = 8\text{Hz}$), $7.58\text{-}7.54$ (m, 2H), 7.17 (t, 2H, $J = 8\text{Hz}$).



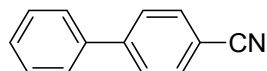
4-Methoxy-2'-methylbiphenyl: **$^1\text{H NMR}$ (400 MHz, CDCl_3 , ppm):** $\delta = 7.25\text{-}7.21$ (m, 6H),
 6.95 (d, 2H, $J = 8\text{Hz}$), 3.85 (s, 3H), 2.27 (s, 3H).



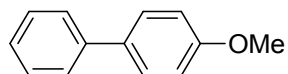
4-Cyano-2'-methylbiphenyl: **$^1\text{H NMR}$ (400 MHz, CDCl_3 , ppm):** $\delta = 7.69$ (d, 2H, $J = 8\text{Hz}$),
 7.42 (m, 2H), $7.29\text{-}7.26$ (m, 3H), 7.18 (d, 1H, $J = 8\text{ Hz}$), 2.24 (s, 3H).



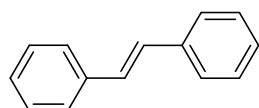
4-Methoxy-2'-fluorobiphenyl: **$^1\text{H NMR}$ (400 MHz, CDCl_3 , ppm):** $\delta = 7.50\text{-}7.45$ (m, 4H),
 7.09 (t, 2H, $J = 8\text{Hz}$), 6.96 (d, 2H, $J = 8\text{Hz}$), 3.84 (s, 3H).



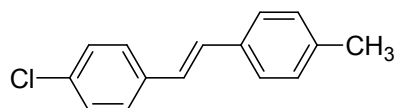
4-Cyanobiphenyl: **$^1\text{H NMR}$ (400 MHz, CDCl_3 , ppm):** $\delta = 7.72\text{-}7.66$ (m, 4H), 7.58 (d, 2H, $J = 8\text{Hz}$),
 7.47 (t, 2H, $J = 8\text{Hz}$), 7.41 (t, 1H, $J = 8\text{Hz}$), **$^{13}\text{C NMR}$ (100 MHz, CDCl_3 , ppm):**
 $145.6, 139.1, 132.6, 129.1, 128.6$ $127.7, 127.2, 118.9, 110.8$.



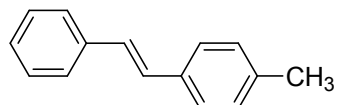
4-Methoxybiphenyl: **¹H NMR (400 MHz, CDCl₃, ppm):** δ = 7.50 (t, 4H, *J* = 8Hz), 7.39 (t, 2H, *J* = 8Hz), 7.30 (t, 1H, *J* = 8Hz), 6.96 (d, 2H, *J* = 8Hz), 3.82 (s, 3H), **¹³C NMR (100 MHz, CDCl₃, ppm):** 150.1, 140.8, 133.8, 128.7, 128.2, 126.8, 126.7, 114.2, 55.4



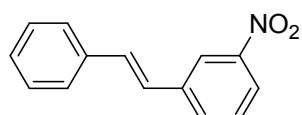
(E)-trans-Stilbene: **¹H NMR (400 MHz, CDCl₃, ppm):** δ = 7.52 (d, 4H, *J* = 8 Hz), 7.36 (t, 4H, *J* = 8 Hz), 7.26 (t, 2H, *J* = 8 Hz), 7.11 (s, 2H).



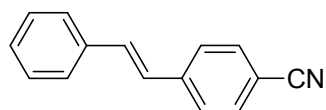
(E)-1-Chloro-4-(4-methylstyryl)benzene: **¹H NMR (400 MHz, CDCl₃, ppm):** δ = 7.41 (t, 4H, *J* = 8 Hz), 7.31 (d, 2H, *J* = 8 Hz), 7.17 (d, 2H, *J* = 8 Hz), 7.02 (d, 2H, *J* = 12 Hz), 2.36 (s, 3H).



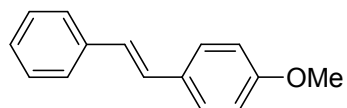
(E)-4-Methyl-trans-stilbene: **¹H NMR (400 MHz, CDCl₃, ppm):** δ = 7.49 (d, 2H, *J* = 8 Hz), 7.40 (d, 2H, *J* = 8 Hz), 7.34 (t, 2H, *J* = 8 Hz), 7.23 (t, 1H, *J* = 8 Hz), 7.15 (d, 2H, *J* = 7.76Hz), 7.06 (s, 2H), 2.35 (s, 3H).



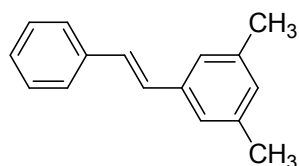
(E)-3-Nitro-trans-stilbene: **¹H NMR (400 MHz, CDCl₃, ppm):** δ = 8.37 (s, 1H), 8.10 (d, 1H, *J* = 8 Hz), 7.80 (d, 1H, *J* = 8 Hz), 7.56-7.50 (m, 3H), 7.40 (t, 2H, *J* = 8 Hz), 7.32 (t, 1H, *J* = 8 Hz), 7.24 (d, 1H, *J* = 16 Hz), 7.14 (d, 1H, *J* = 16 Hz).



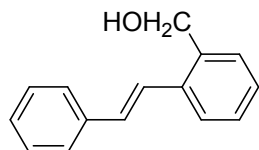
(E)-4-Cyano-trans-stilbene: **$^1\text{H NMR}$ (400 MHz, CDCl_3 , ppm):** $\delta = 7.65\text{-}7.57$ (m, 4H), 7.54 (d, 2H, $J = 8$ Hz), 7.39 (t, 2H, $J = 8$ Hz), 7.32 (t, 1H, $J = 8$ Hz), 7.22 (d, 1H, $J = 16$ Hz), 7.09 (d, 1H, $J = 16$ Hz).



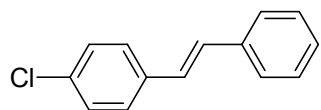
(E)-4-Methoxy-trans-stilbene: **$^1\text{H NMR}$ (400 MHz, CDCl_3 , ppm):** $\delta = 7.49\text{-}7.44$ (m, 4H), 7.34 (t, 2H, $J = 8$ Hz), 7.23 (t, 1H, $J = 8$ Hz), 7.06 (d, 1H, $J = 16$ Hz), 6.97 (d, 1H, $J = 16$ Hz), 6.90 (d, 2H, $J = 8$ Hz), 3.82 (s, 3H).



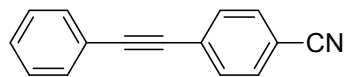
(E)-3,3-Dimethyl-trans-stilbene: **$^1\text{H NMR}$ (400 MHz, CDCl_3 , ppm):** $\delta = 7.50$ (d, 2H, $J = 8$ Hz), 7.34 (t, 2H, $J = 8$ Hz), 7.24 (t, 1H, $J = 8$ Hz), 7.14 (s, 2H), 7.07-7.06 (m, 2H), 6.91 (s, 1H), 2.33 (s, 6H), **$^{13}\text{C NMR}$ (100 MHz, CDCl_3 , ppm):** 138.13, 137.54, 137.25, 129.44, 128.91, 128.66, 128.31, 127.47, 126.46, 124.44, 21.32.



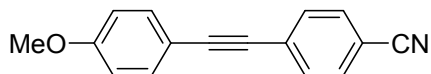
(E)-2-Methanol-trans-stilbene: **$^1\text{H NMR}$ (400 MHz, CDCl_3 , ppm):** $\delta = 7.66$ (d, 1H, $J = 8$ Hz), 7.53 (d, 2H, $J = 8$ Hz), 7.46 (d, 1H, $J = 16$ Hz), 7.40-7.25 (m, 6H), 7.05 (d, 1H, $J = 16$ Hz), 4.84 (s, 2H), 1.65 (s, 1H), **$^{13}\text{C NMR}$ (100 MHz, CDCl_3 , ppm):** 137.81, 137.35, 136.37, 131.23, 128.70, 128.59, 128.32, 127.83, 127.75, 126.70, 125.98, 125.33, 63.66.



(E)-4-Chloro-trans-stilbene: **¹H NMR (400 MHz, CDCl₃, ppm):** δ = 7.50 (d, 2H, *J* = 8 Hz), 7.44 (d, 2H, *J* = 8 Hz), 7.38-7.25 (m, 5H), 7.06 (s, 2H).

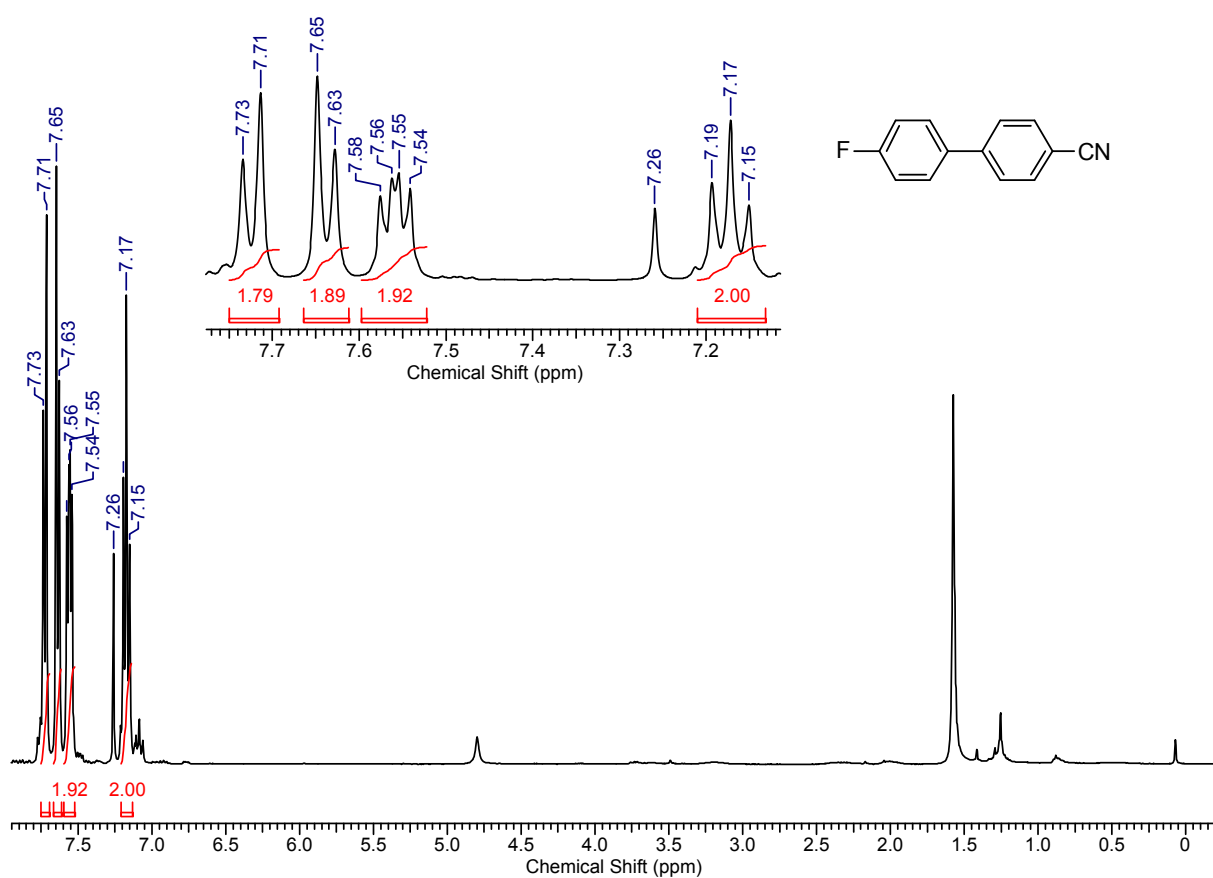


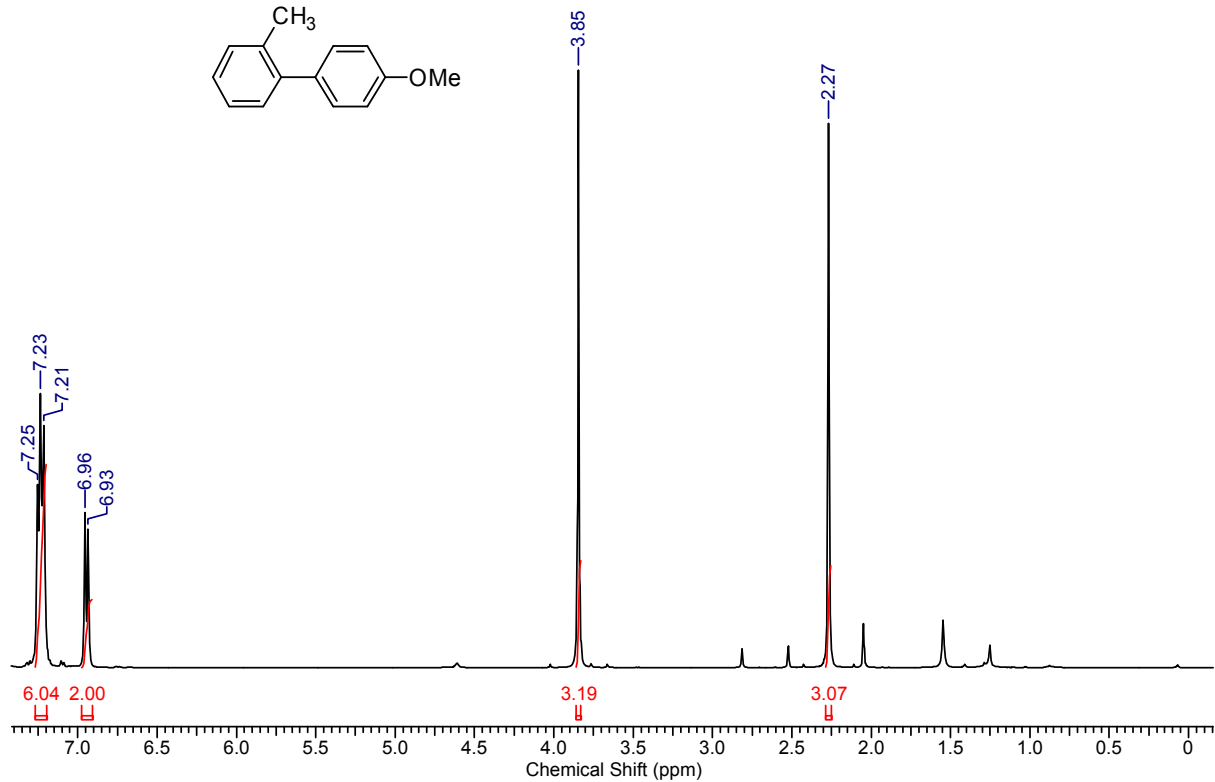
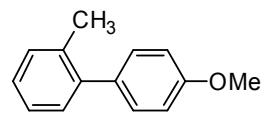
4-(Phenylethynyl)benzonitrile: **¹H NMR (400 MHz, CDCl₃, ppm):** δ = 7.65-7.59 (m, 4H), 7.55-7.54 (m, 2H), 7.39 (s, 3H), **¹³C NMR (100 MHz, CDCl₃, ppm):** 132.03, 132.01, 131.75, 129.69, 128.47, 128.22, 122.18, 118.50, 111.43, 93.75, 87.69.

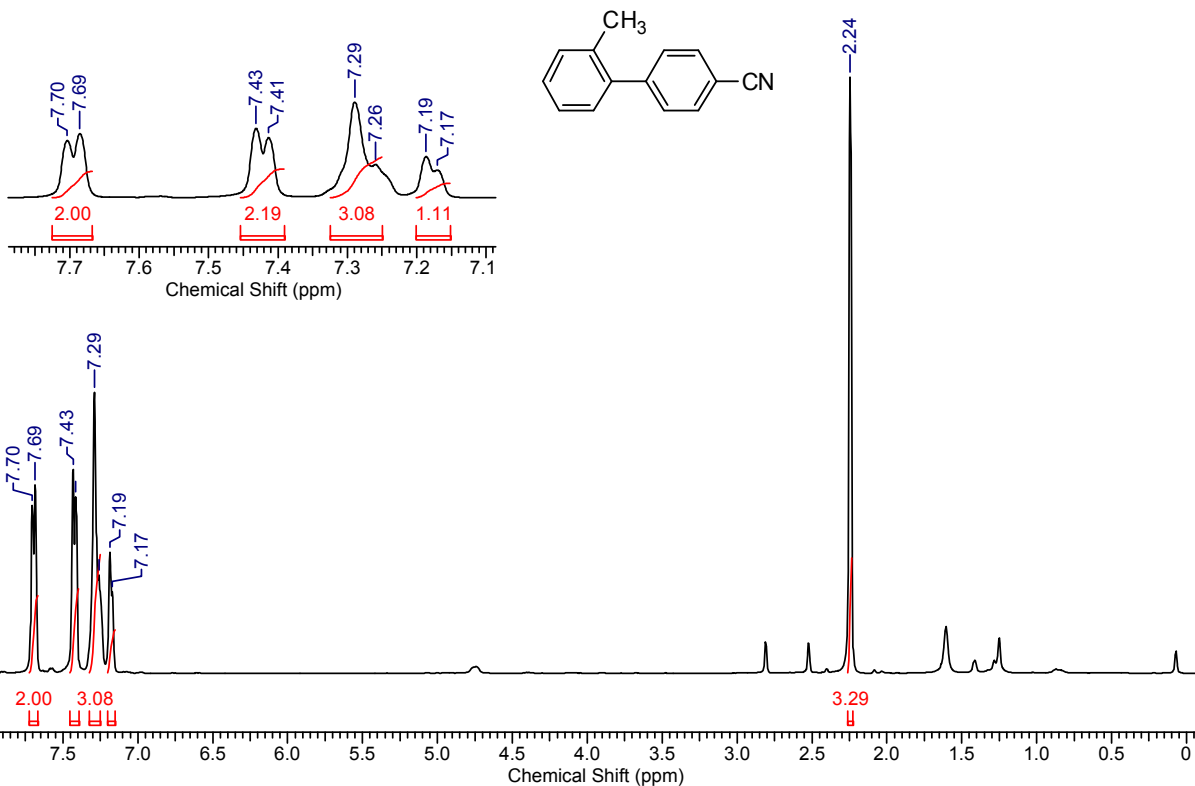


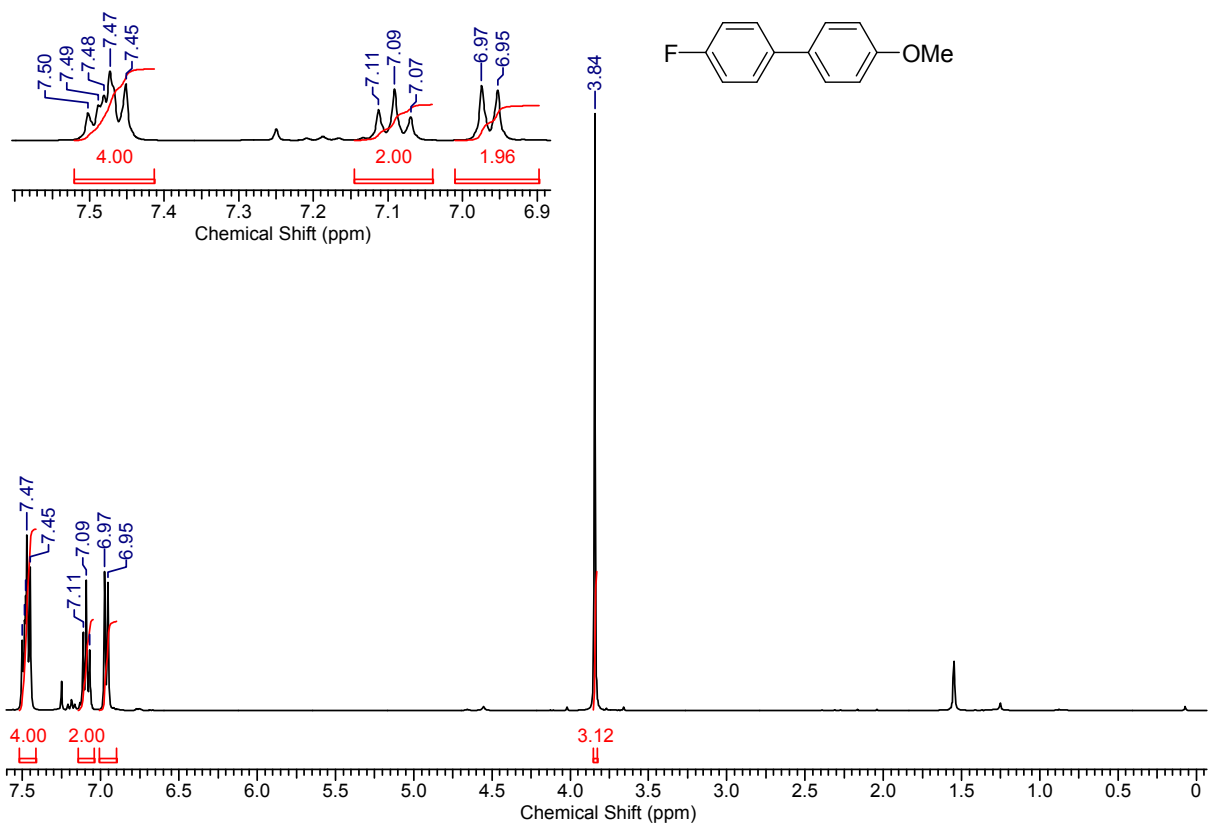
4-((4-Methoxyphenyl)ethynyl)benzonitrile: **¹H NMR (400 MHz, CDCl₃, ppm):** 7.63-7.56 (m, 4H), 7.48 (d, 2H, *J* = 8 Hz), 6.90 (d, 2H, *J* = 8 Hz), 3.84 (s, 3H).

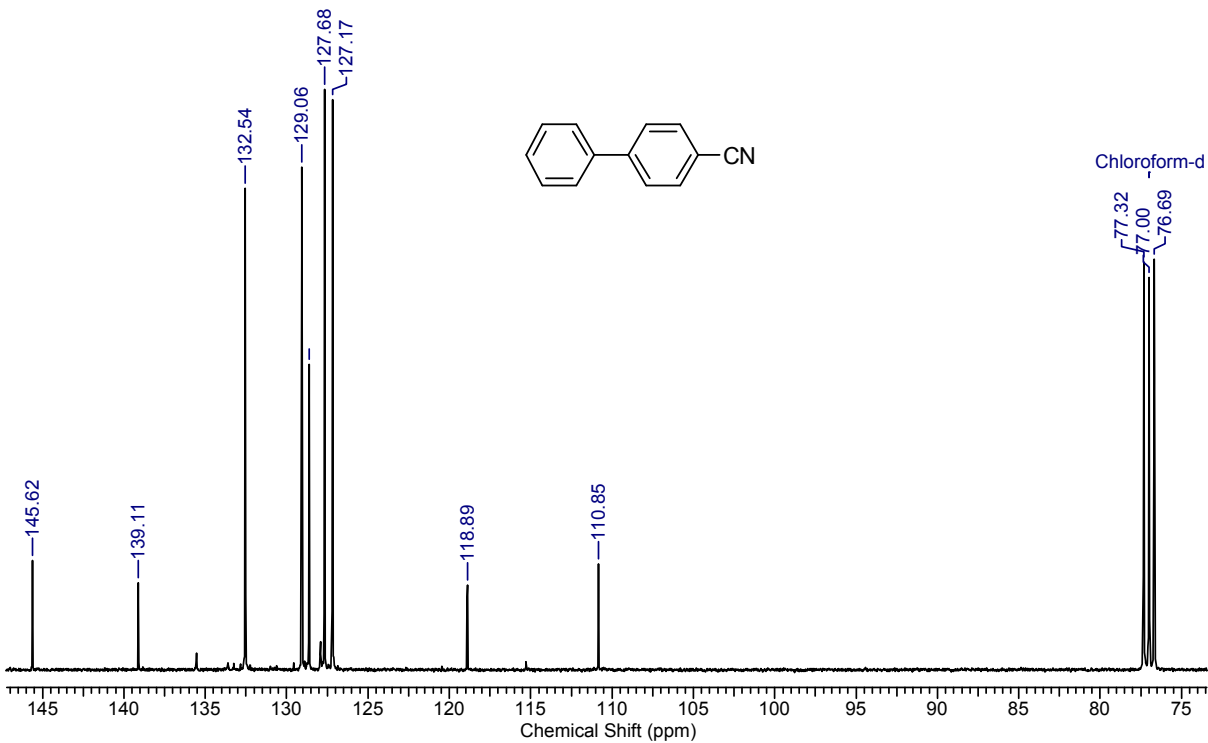
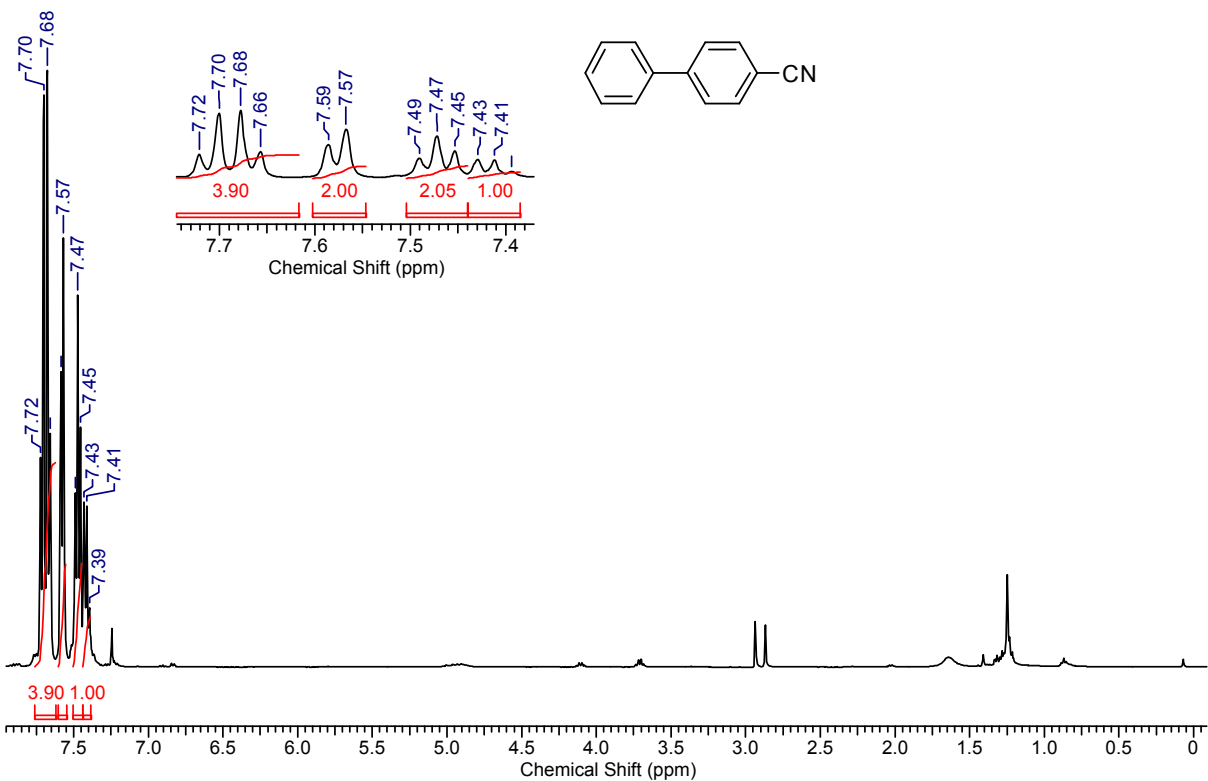
Spectra of the coupled products

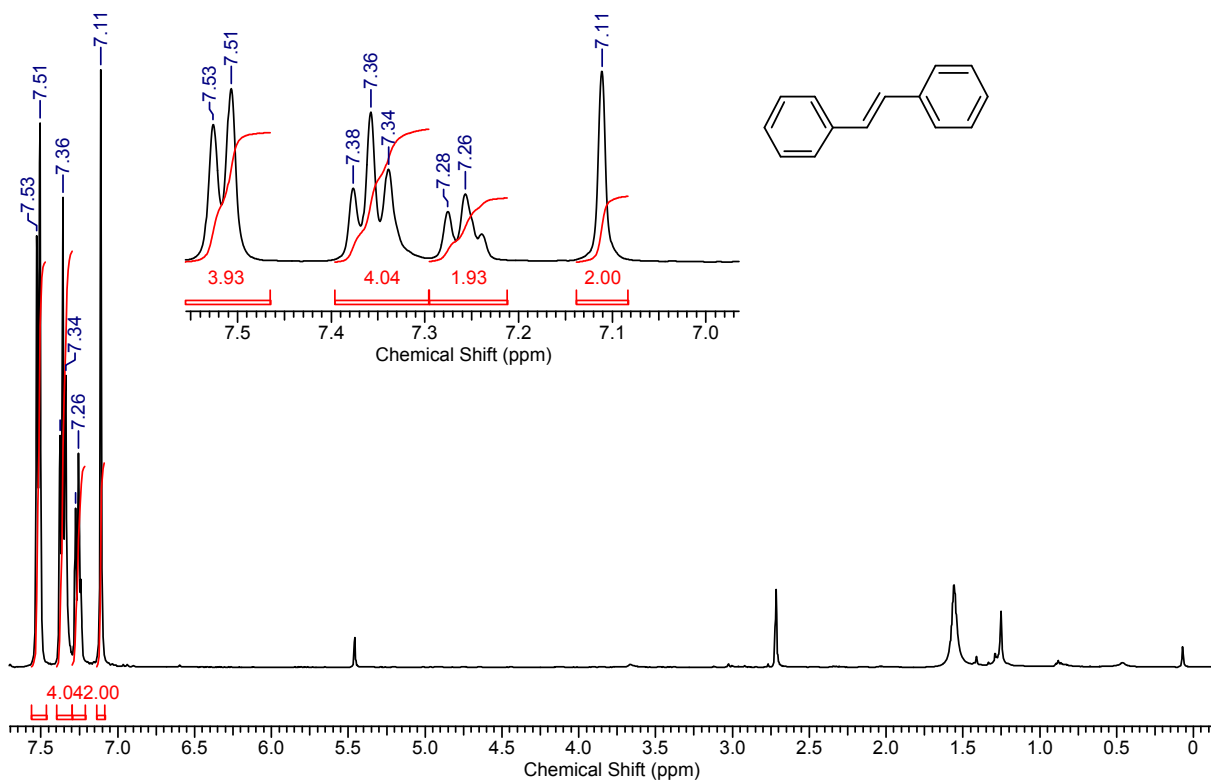


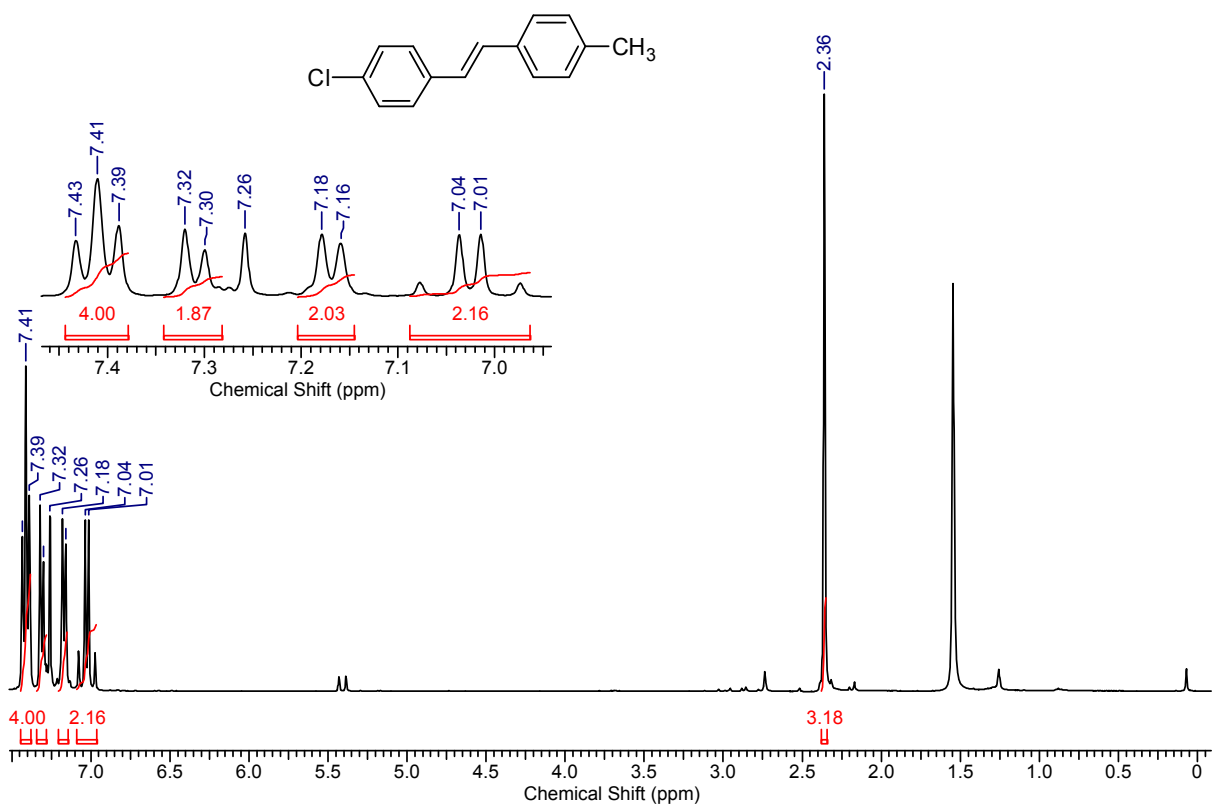


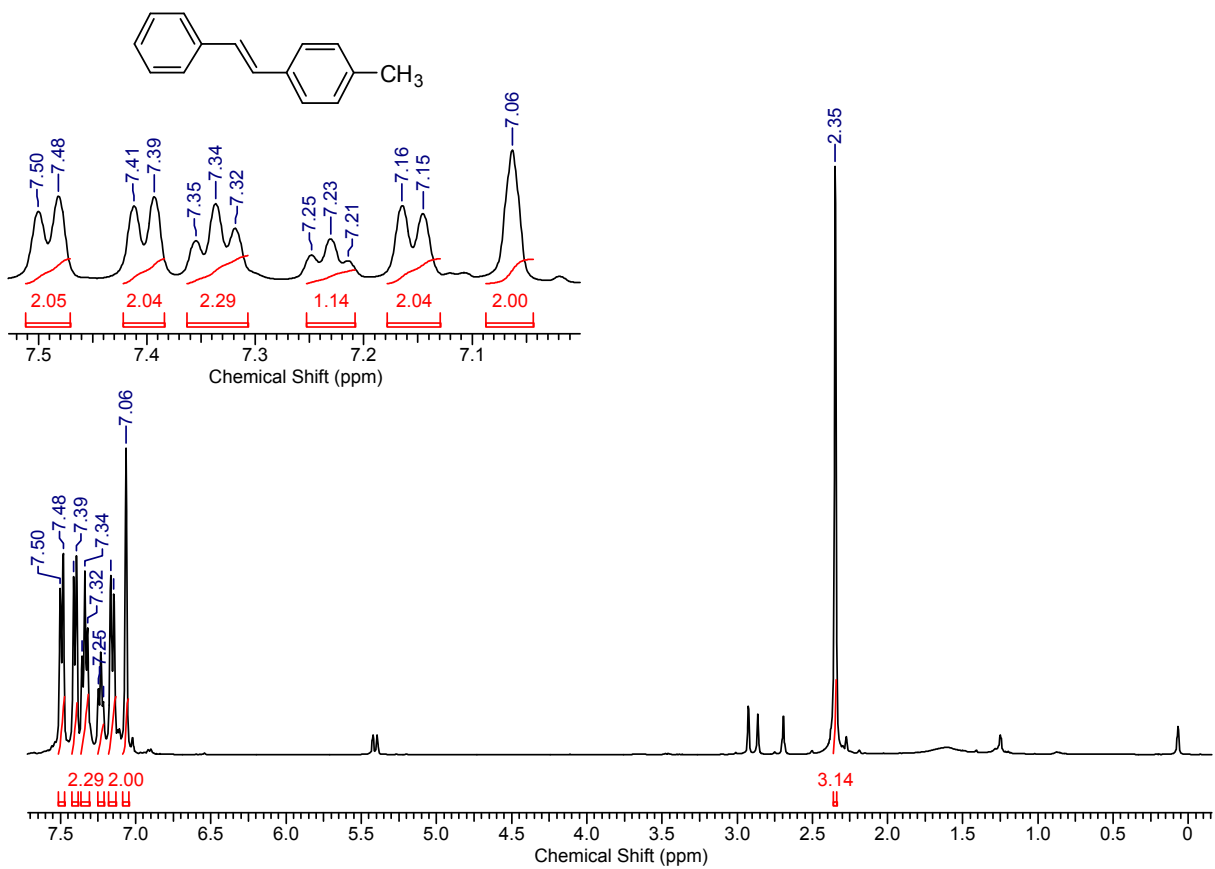


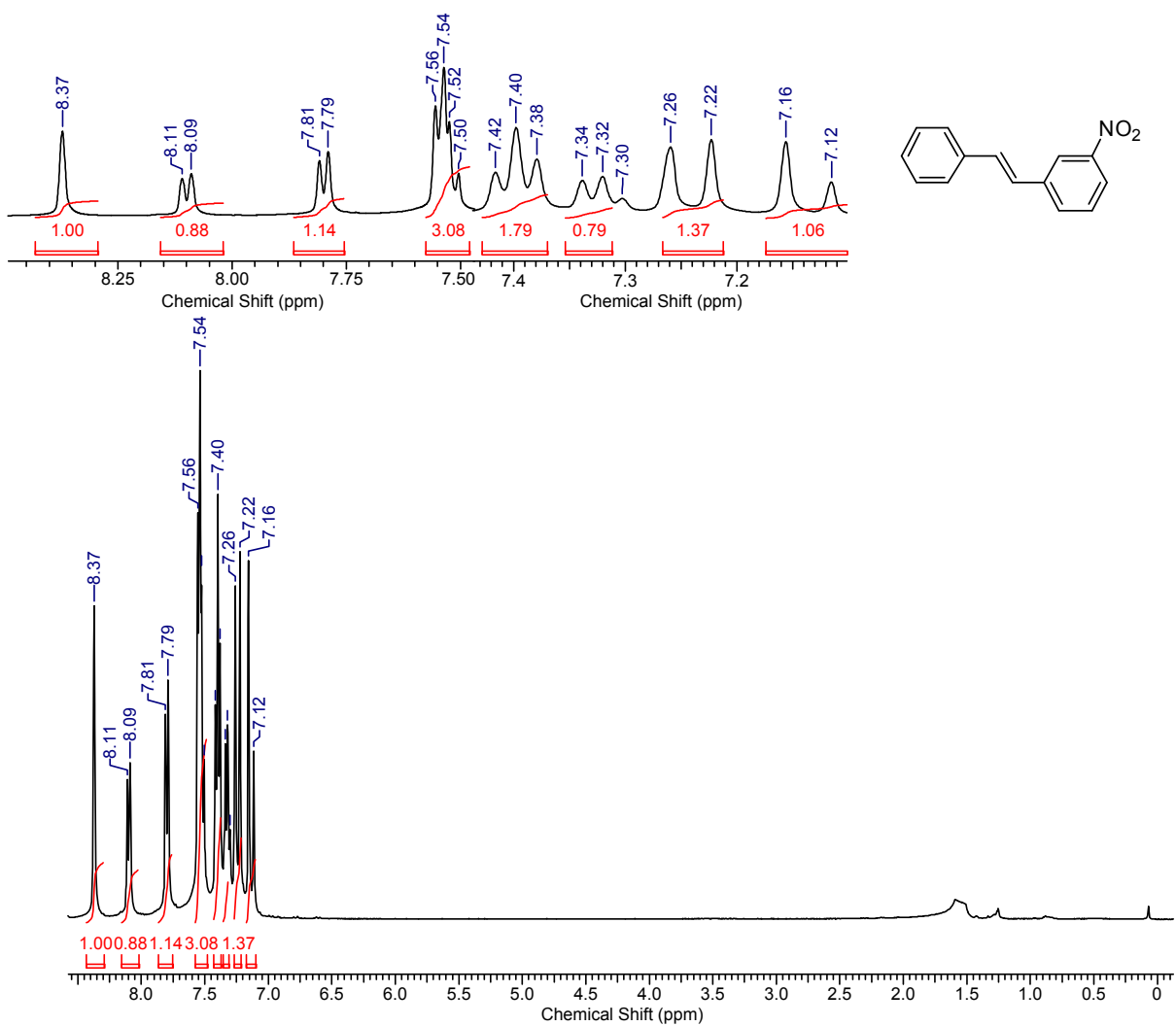


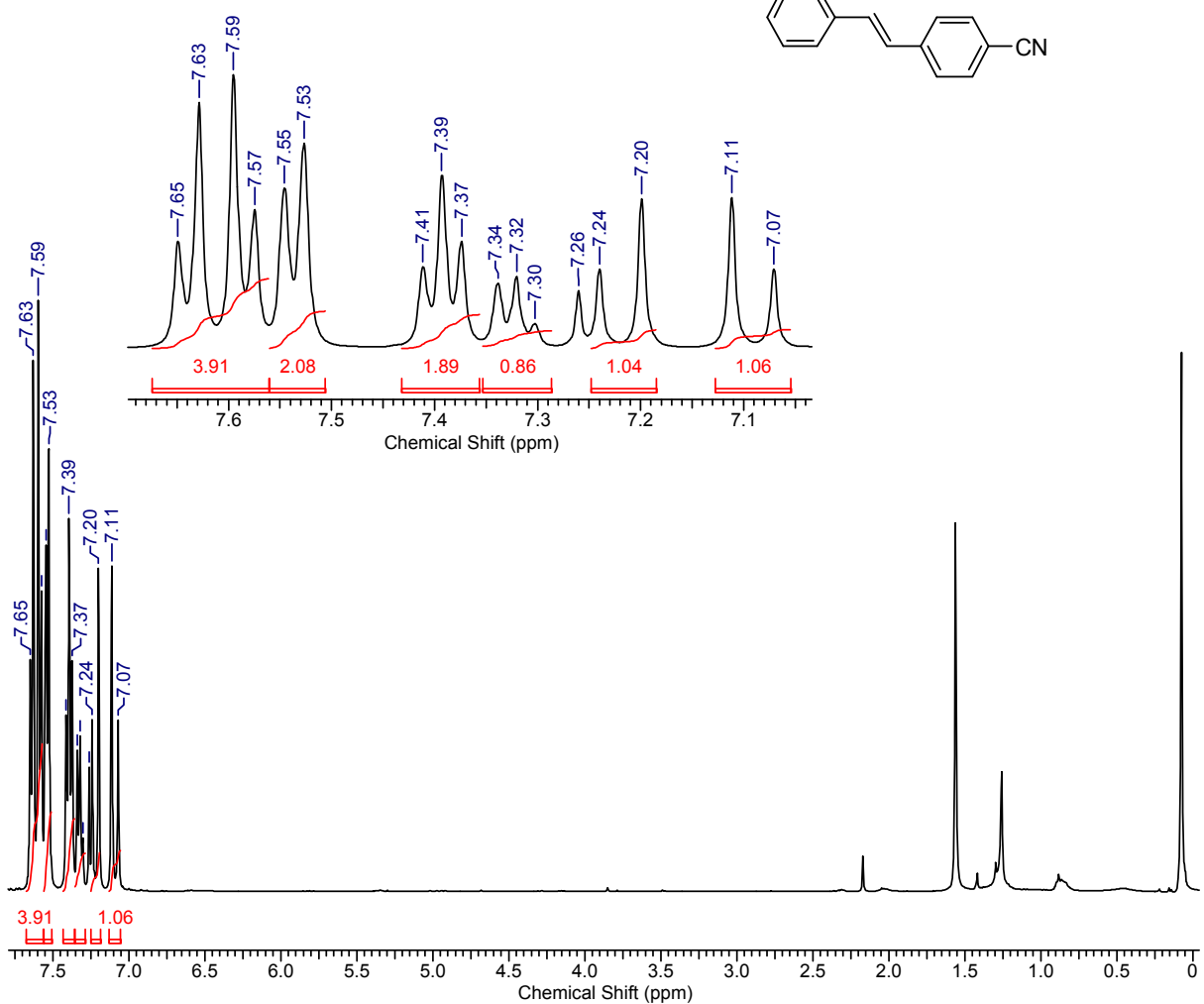
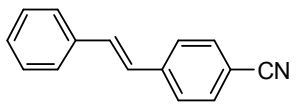


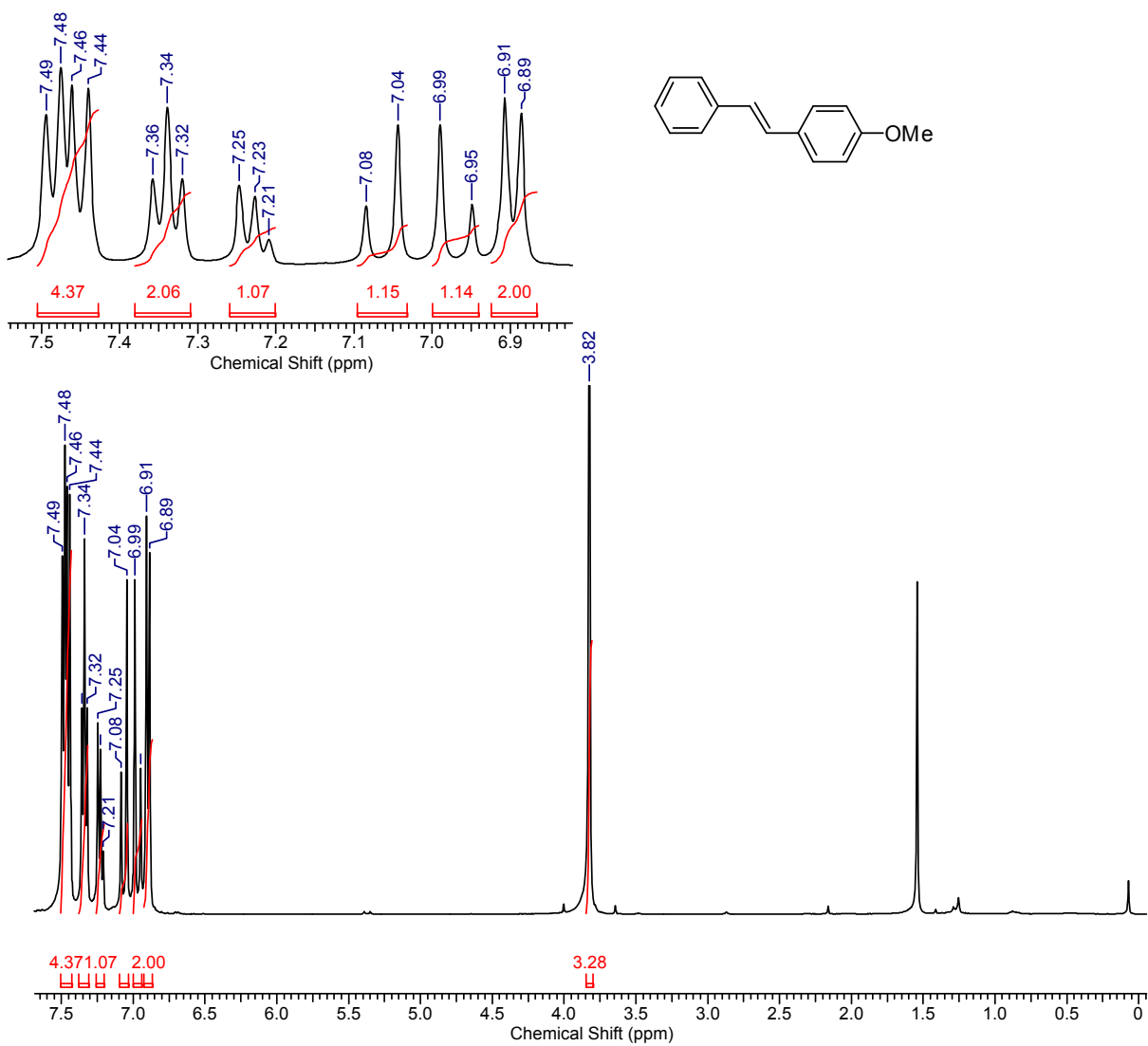


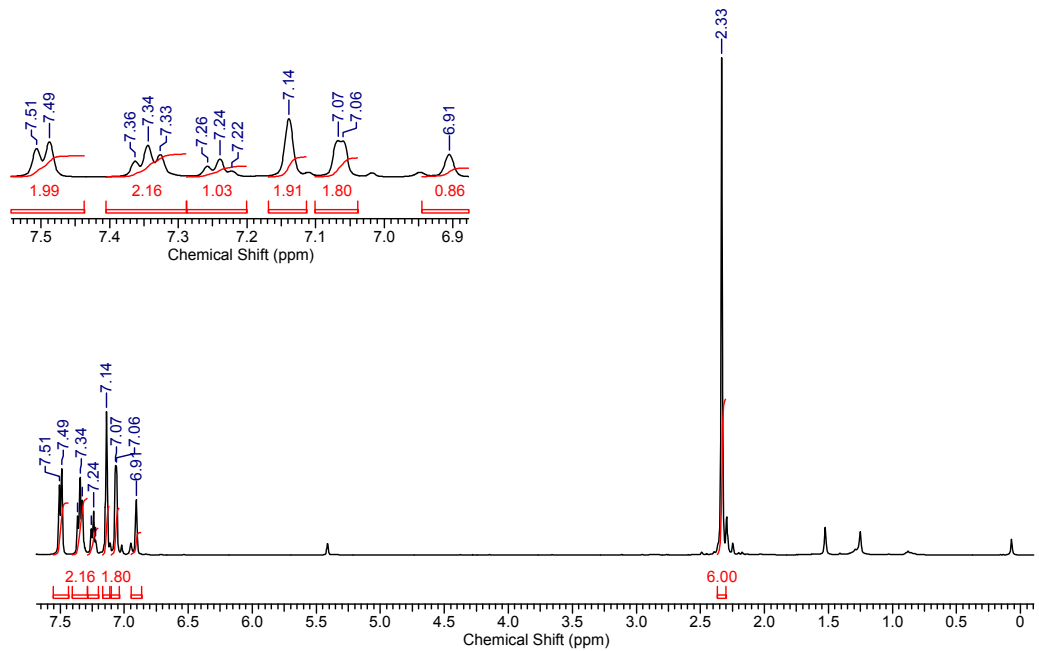
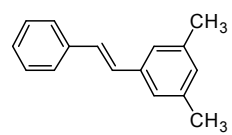


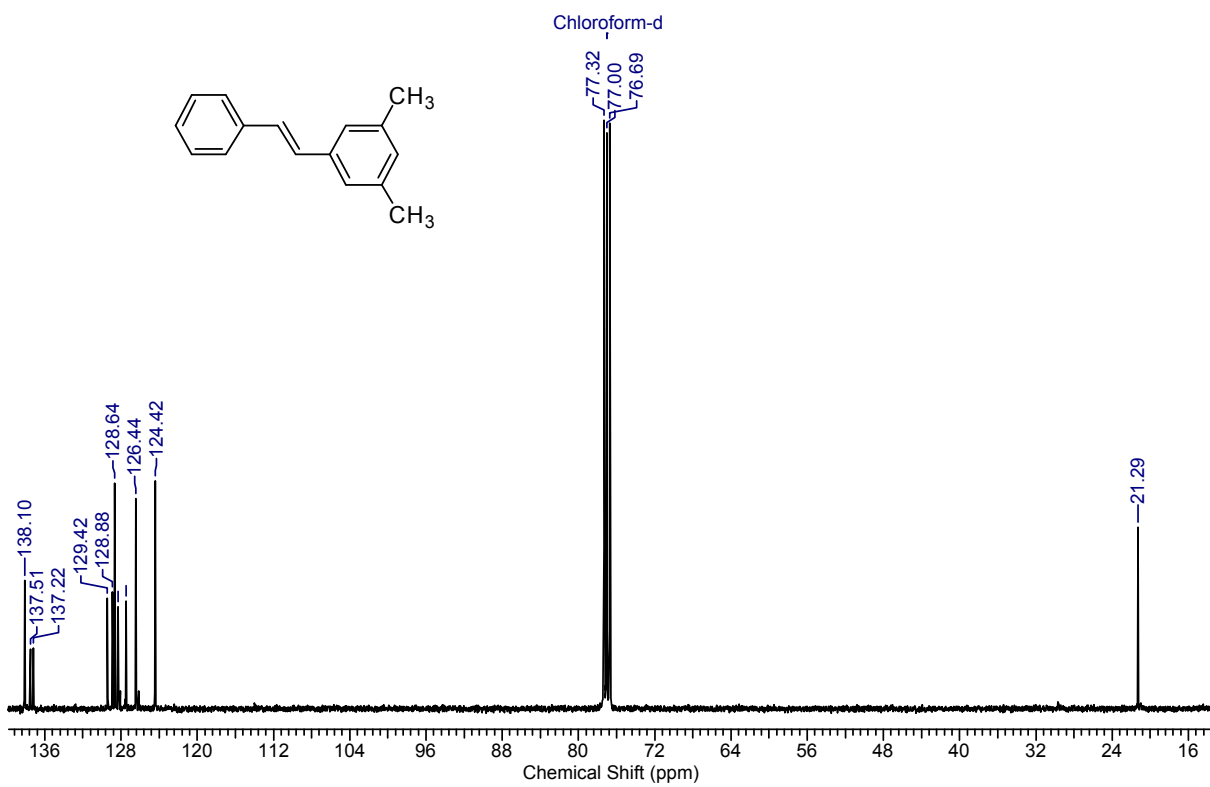


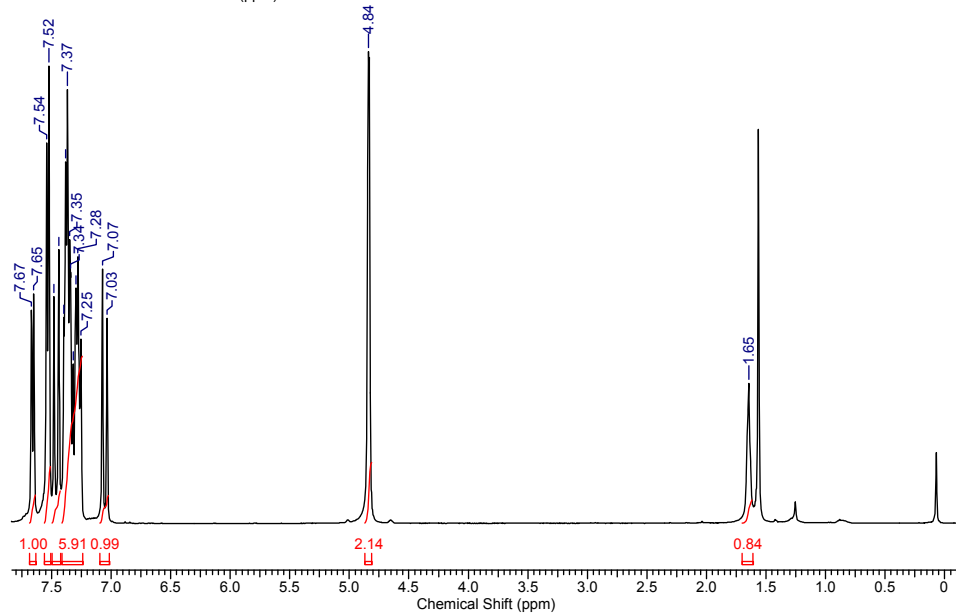
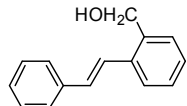
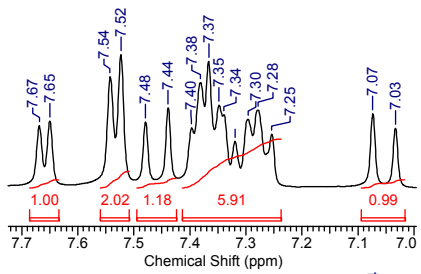


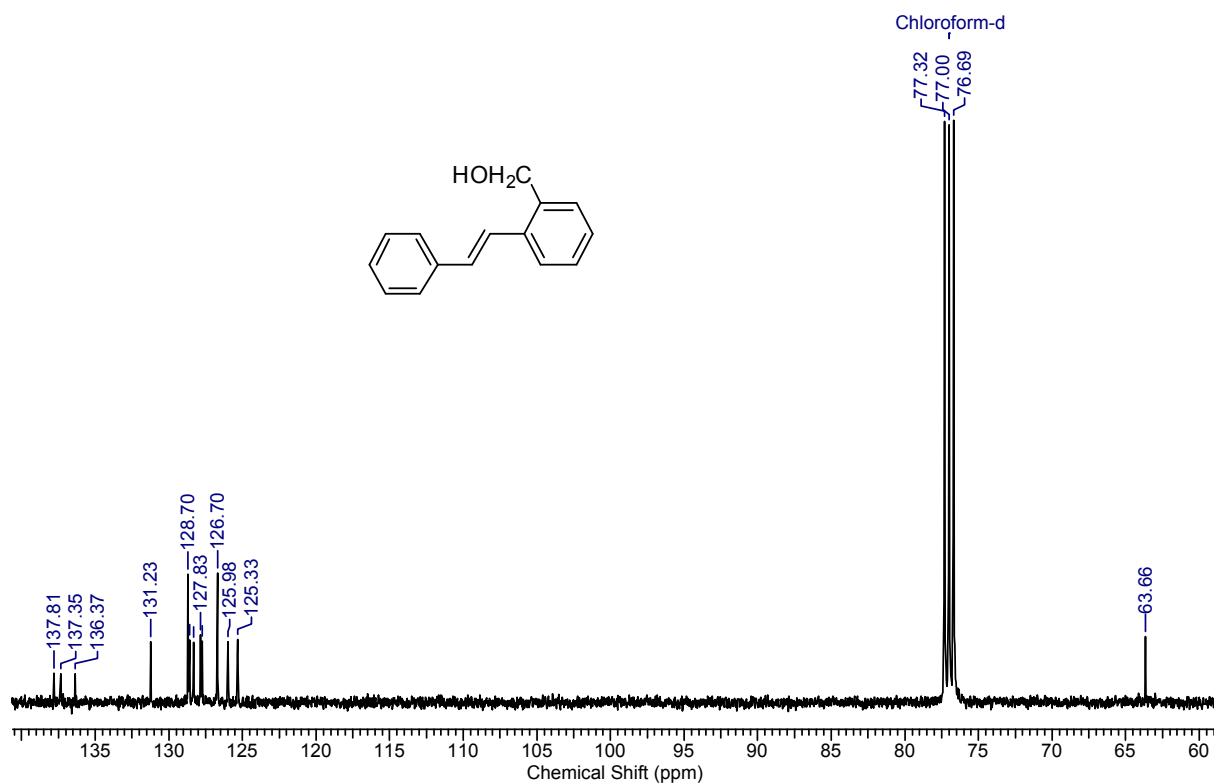


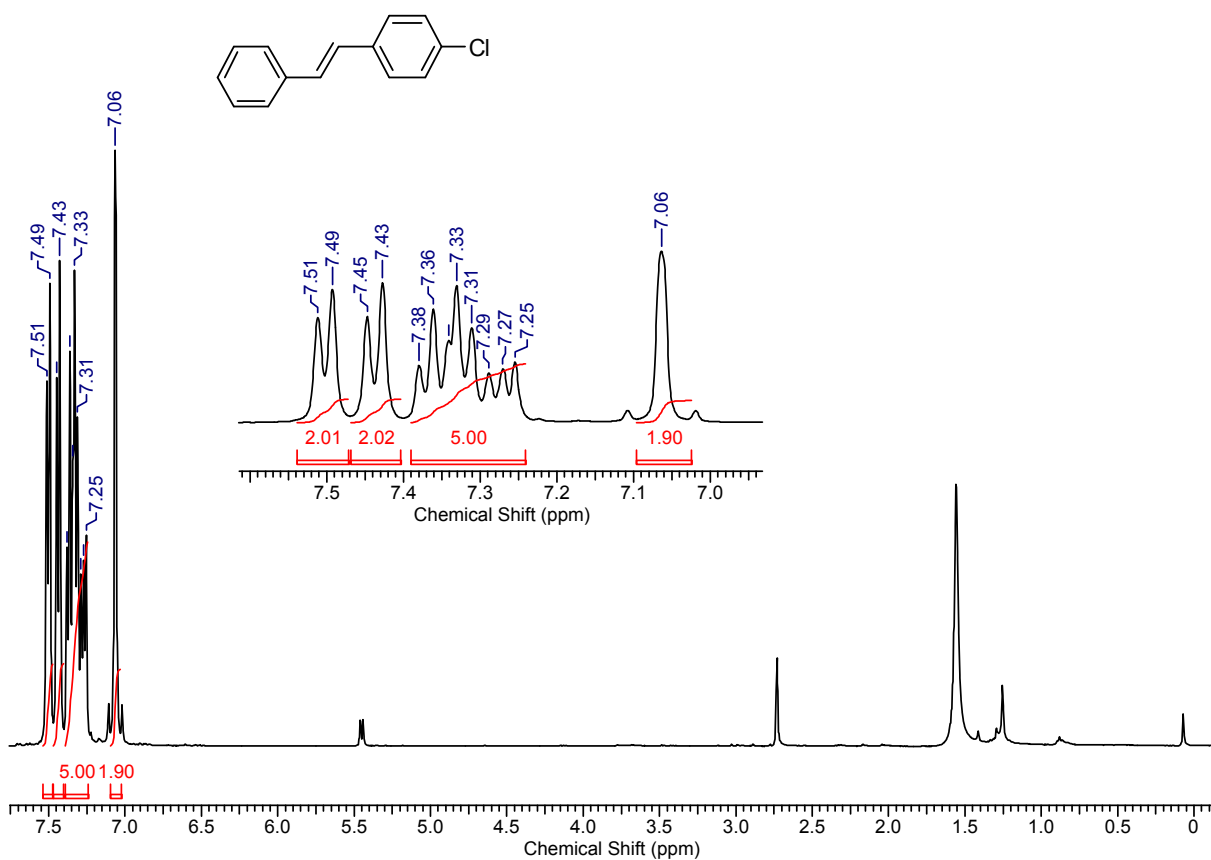


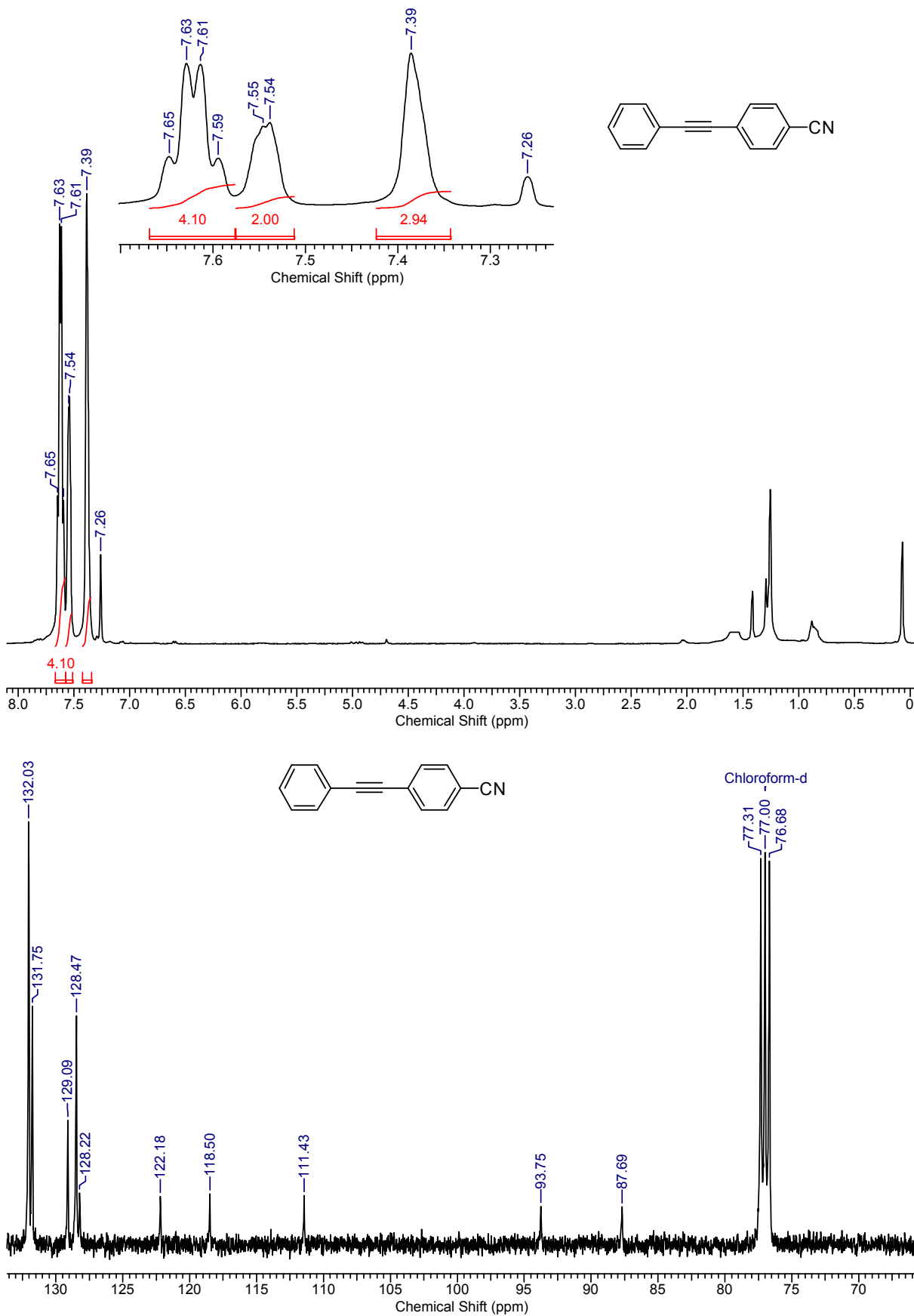












References

- S1 A. Mahata, R. K. Rai, I. Choudhuri, S. K. Singh and B. Pathak, *Phys. Chem. Chem. Phys.*, 2014, **16**, 26365-26374.
- S2 I. Choudhuri, N. Patra, A. Mahata, R. Ahuja and B. Pathak *J. Phys. Chem. C*, 2015, **119**, 24827-24836.
- S3 J. Saha, K. Bhowmik, I. Das and G. De, *Dalton Trans.*, 2014, **43**, 13325-13332.
- S4 K. Seth, P. Purohit and A. K. Chakraborti, *Org. Lett.*, 2014, **16**, 2334-2337.
- S5 Y. Wu, D. Wang, P. Zhao, Z. Niu, Q. Peng and Y. Li, *Inorg. Chem.*, 2011, **50**, 2046-2048.
- S6 J. Xiang, P. Li, H. Chong, L. Feng, F. Fu, Z. Wang, S. Zhang and M. Zhu, *Nano Res.*, 2014, **7**, 1337-1343.
- S7 Ö. Metin, S. F. Ho, C. Alp, H. Can, M. N. Mankin, M. S. Gultekin, M. Chi and S. Sun, *Nano Res.*, 2013, **6**, 10-18.
- S8 M. T. Reetz, R. Breinbauerm and K. Wanniger, *Tetrahedron Lett.*, 1996, **37**, 4499-4502.
- S9 A. Ohtaka, J. M. Sansano, C. Nájera, I. Miguel-García, A. Berenguer-Murcia and D. Cazorla-Amorós, *ChemCatChem*, 2015, **7**, 1841-1847.
- S10 M. Gholinejad, M. Razeghi, A. Ghaderi and P. Bijji, *Catal. Sci. Technol.*, DOI: 10.1039/c5cy00821b.
- S11 R. Fareghi-Alamdari, M. G. Haqiqib and N. Zekri, *New J. Chem.*, 2016, **40**, 1287-1296.
- S12 J. Hu, Y. Wang, M. Han, Y. Zhou, X. Jiang and P. Sun, *Catal. Sci. Technol.*, 2012, **2**, 2332-2340.
- S13 M. Nasrollahzadeh and S. M. Sajadi, *J. Colloid Interface Sci.*, 2016, **465**, 121-127.

- S14 N. Hussain, A. Borah, G. Darabdhara, P. Gogoi, V. K. Azhagan, M. V. Shelke and M. R. Das, *New J. Chem.*, 2015, **39**, 6631-6641.
- S15 H.-Q. Song, Q. Zhu, X.-S Zheng and X. Q. Chen, *J. Mater. Chem. A*, 2015, **3**, 10368-10377.
- S16 H. Yuan, H. Y. Liu, B. S. Zhang, L. Y. Zhang, H. H. Wang and D. S. Su, *Phys. Chem. Chem. Phys.*, 2014, **16**, 11178-11181.
- S17 S. Yamamoto, H. Kinoshita, H. Hashimoto and Y. Nishina, *Nanoscale*, 2014, **6**, 6501-6505.
- S18 M. Nasrollahzadeh, S. M. Sajadi, A. Rostami-Vartooni and M. Khalaj, *J. Mol. Catal. A: Chem.*, 2015, **396**, 31-35.
- S19 A. R. Siamaki, Y. Lin, K. Woodberry, J. W. Connell and B. F. Gupton, *J. Mater. Chem. A*, 2013, **1**, 12909-12918.
- S20 F. Costantino, R. Vivani, M. Bastianini, L. Ortolani, O. Piermatti, M. Nocchetti and L. Vaccaro, *Chem. Commun.*, 2015, **51**, 15990-15993.
- S21 P. Ncube, T. Hlabathe and R. Meijboom, *J. Clust. Sci.*, 2015, **26**, 1873-1888.
- S22 F. Chen, M. Huang and Y. Li, *Ind. Eng. Chem. Res.*, 2014, **53**, 8339-8345.
- S23 J. C. Park, E. Heo, A. Kim, M. Kim, K. H. Park and H. Song, *J. Phys. Chem. C*, 2011, **115**, 15772-15777.
- S24 S. R. Borhade and S. B. Waghmode, *Beilstein J. Org. Chem.* 2011, **7**, 310-319.
- S25 S. Zhou, M. Johnson and J. G. C. Veinot, *Chem. Commun.*, 2010, **46**, 2411-2413.
- S26 M. Chtchigrovsky, Y. Lin, K. Ouchouaou, M. Chaumontet, M. Robitzer, F. Quignard and F. Taran, *Chem. Mater.*, 2012, **24**, 1505-1510.
- S27 E. Rafiee, M. Kahrizi, M. Joshaghani, P. G.-S. Abadi, *Res. Chem. Intermed.*, DOI: 10.1007/s11164-015-2387-5.

- S28 L. Zhang, Z. Su, F. Jiang, Y. Zhou, W. Xu and M. Hong, *Tetrahedron*, 2013, **69**, 9237-9244.
- S29 J. Wang, B. Xu, H. Sun, G. Song, *Tetrahedron Lett.*, 2013, **54**, 238-241.
- S30 H. Joshi, K. N. Sharma, A. K. Sharma and A. K. Singh, *Nanoscale*, 2014, **6**, 4588-4597.
- S31 P. M. Uberman, L. A. Perez, S. E. Martin and G. I. Lacconi, *RSC Adv.*, 2014, **4**, 12330-12341.